JGR Earth Surface

RESEARCH ARTICLE
10.1029/2024JF007740

Impacts of Post-Fire Debris Flows on Fluvial Morphology and Sediment Transport in a California Central Coast Stream

Telemak Olsen[1], Allison M. Pfeiffer[1], Noah J. Finnegan[2], Chuxuan Li[3], and Daniel E. Horton[3]

[1]Department of Geology, Western Washington University, Bellingham, WA, USA, [2]Department Earth and Planetary Sciences, University of California-Santa Cruz, Santa Cruz, CA, USA, [3]Department of Earth, Environmental, and Planetary Sciences, Northwestern University, Evanston, IL, USA

Key Points:

- Debris flows reorganized the step structure in Big Creek and triggered substantial grain size fining
- Modeling indicates that grain size fining and discharge increases led to an increase in bedload transport in Big Creek 1 year post-fire
- Debris flows formed a log jam upstream of our Big Creek study reach, which spurred grain size recovery 2 years post-fire

Supporting Information:

Supporting Information may be found in the online version of this article.

Correspondence to:

T. Olsen,
telemakolsen@gmail.com

Citation:

Olsen, T., Pfeiffer, A. M., Finnegan, N. J., Li, C., & Horton, D. E. (2024). Impacts of post-fire debris flows on fluvial morphology and sediment transport in a California central coast stream. *Journal of Geophysical Research: Earth Surface*, *129*, e2024JF007740. https://doi.org/10.1029/2024JF007740

Received 14 MAR 2024
Accepted 18 NOV 2024

Author Contributions:

Conceptualization: Telemak Olsen, Allison M. Pfeiffer
Formal analysis: Telemak Olsen, Allison M. Pfeiffer
Funding acquisition: Telemak Olsen, Allison M. Pfeiffer
Investigation: Telemak Olsen, Allison M. Pfeiffer
Methodology: Telemak Olsen, Allison M. Pfeiffer, Chuxuan Li, Daniel E. Horton
Resources: Allison M. Pfeiffer
Supervision: Allison M. Pfeiffer
Validation: Telemak Olsen, Allison M. Pfeiffer
Visualization: Telemak Olsen
Writing – original draft: Telemak Olsen
Writing – review & editing: Telemak Olsen, Allison M. Pfeiffer, Chuxuan Li, Daniel E. Horton

Abstract Post-fire debris flows alter impacted fluvial systems, but few studies quantify the magnitude and timing of reach-scale channel response to these events. In August 2020, the Big Creek watershed along California's central coast burned in the Dolan Fire; in January 2021, an atmospheric river event triggered post-fire debris flows in steep tributaries to the Big Creek. Here, we characterize the evolution of fluvial morphology and grain size in Big Creek, a cascade and step-pool channel downstream of tributaries in which post-fire debris flows initiated, using pre- and post-fire structure from motion (SfM) and airborne lidar surveys. We also make comparisons to Devil's Creek, an adjacent basin which burned but did not experience post-fire debris flows. We observe grain size fining following debris flows in Big Creek, but the coarsest 40% of the grain size distribution remained essentially unchanged despite reorganization of channel structure. Changes in grain size and elevated post-fire peak flows account for approximately equal portions of a substantial increase in modeled bedload transport capacity one year post-fire. In Big Creek, geomorphic recovery is well underway just two years post-fire. A valley-spanning log jam, which formed during debris flows, acts as a sediment trap upstream of our Big Creek study reach, and is partially responsible for accelerating recovery processes. In contrast, Devil's Creek exhibited little change in morphology or grain size despite elevated post-fire peak flows. This period of geomorphic dynamism following the Dolan Fire has complex ecological impacts, notably for the threatened anadromous salmonid spawning habitat in Big Creek.

Plain Language Summary Wildfires destroy vegetation and impair soils' ability to absorb rainfall. Fast-moving mixtures of water and sediment (called debris flows) often flow through steep stream channels during storms following wildfires. Debris flows alter the form of affected streams and introduce large volumes of sediment to channels downstream. We document changes in the form and behavior of Big Creek, a stream in Big Sur, California which experienced debris flows after the 2020 Dolan Fire. We make comparisons to Devil's Creek, an adjacent stream which did not experience debris flows. Debris flows introduced additional fine sediment to Big Creek. Computer modeling indicates that this decrease in average grain size, coupled with increases in streamflow, led to an increase in the volume of sediment transported in Big Creek one year after the wildfire. Two years after the wildfire, the grain size in Big Creek had coarsened. We interpret coarsening as recovery toward pre-fire conditions, and suggest that a newly formed log jam upstream of our study area acts to trap sediment supplied from upstream, accelerating recovery toward pre-fire conditions. In contrast, grain size in Devil's Creek remained relatively consistent throughout our study period. Post-fire changes in Big Creek have implications for threatened fish habitats.

1. Introduction

Debris flows shape headwater channels in steep landscapes and deliver large volumes of sediment to downstream fluvial systems (Lisle, 1987; Montgomery & Buffington, 1997; Stock & Dietrich, 2006). Step-pool channels often exist within debris flow transport zones; in these transport reaches, debris flows transport boulders and large wood, thereby adjusting step-pool configuration (Lisle, 1987; Montgomery & Buffington, 1997). In the lower reaches of steep basins, debris flows cause episodic increases in sediment supply. Increases in sediment supply are commonly associated with bed surface grain size fining, elevated bedload transport rates, and aggradation (Dietrich et al., 1989; Wang et al., 2021). In steep channels, step-pool configuration is highly dynamic in response to sediment pulses, with steps and pools both forming and collapsing more frequently during and after sediment

pulses (Wang et al., 2021). Increases in sediment supply are also associated with deposition of fine sediment in pools at low flow as winnowed grains from upstream accumulate (Lisle & Hilton, 1992). As sediment supply wanes following major sediment input, the bed surface coarsens, which stabilizes channels and regulates sediment transport (Gran & Montgomery, 2005). Notably, morphological changes from sediment supply perturbations impact anadromous salmonids, for which spawning success is highly dependent on substrate characteristics (Kondolf & Wolman, 1993; Riebe et al., 2014).

Wildfire increases total runoff, streamflow volume, and peak flow magnitude via a variety of mechanisms. Wildfire removes vegetation and litter from the burned landscape, reducing total evapotranspiration in addition to water and sediment storage capacity and increasing runoff and hillslope sediment yield (DiBiase & Lamb, 2013; Lamb et al., 2013; Loáiciga et al., 2001; Stoof et al., 2012). Wildfire may also induce soil-water repellency, reducing permeability and infiltration capacity, which promotes erosive overland flow on burned hillslopes (DeBano, 2000; Gabet & Sternberg, 2008; MacDonald & Huffman, 2004). Hydrologic response to wildfires is locally heterogeneous; the magnitude and recovery timescales of hydrologic responses to wildfires largely depend on burn severity and basin characteristics, including vegetation type, soil characteristics, and human management (de Jonge et al., 1999; DeBano, 2000; Ice et al., 2004; MacDonald & Huffman, 2004). These changes in basin hydrology induce and exacerbate potential geomorphic responses to wildfires, including debris flows, as exemplified in Big Creek following the Dolan fire.

In California, anthropogenic climate change has and will continue to spur shifts toward increasingly wildfire-prone climate conditions. Warmer conditions are associated with meteorological and agricultural drought, or precipitation and soil moisture deficits, which contribute to vegetation mortality and drying (AghaKouchak et al., 2023; Diffenbaugh et al., 2015; Williams et al., 2015). Moreover, California is experiencing more frequent and intense precipitation events in winter, which exacerbate the geomorphic response to wildfires (Cayan et al., 2008; East & Sankey, 2020; Florsheim et al., 2017; Persad et al., 2020; Swain et al., 2018; Williams et al., 2019). While post-fire debris flows are a natural phenomenon to which many ecosystems have adapted, the increased frequency of these disturbances presents a potential challenge to human infrastructure and aquatic ecosystems.

As fire continues to exert a progressively greater impact on landscapes in the Western U.S., research examining the geomorphic implications of wildfire will become increasingly important in evaluating potential impacts on physical habitat and human infrastructure. While previous studies explore the mechanics of post-fire debris flows (Cannon, 2001; McGuire et al., 2017; Meyer & Wells, 1997), sediment recruitment (DiBiase & Lamb, 2020; Florsheim et al., 1991; Lamb et al., 2013; Morell et al., 2021; Nyman et al., 2015) and spatial patterns in debris flow erosion and deposition (Cenderelli & Kite, 1998; Morell et al., 2021; Rengers et al., 2021), opportunities to conduct highly detailed examinations surrounding the impacts of post-fire debris flows on reach- and bedform-scale channel morphology and dynamics are rare due to a lack of high-resolution pre-fire baseline data. Examples of previous work which used extensive pre- and post-disturbance field data to quantify channel change in response to debris flows include Hoffman and Gabet (2007), and Short et al. (2015). These studies characterized downstream channel response to post-fire debris flows and examined the role of large wood in storing post-fire sediment following a 2001 wildfire in southwestern Montana, but did not compare post-disturbance morphologic data to a pre-fire baseline.

The 2020 Dolan fire and subsequent debris flows in the Big Creek watershed present a unique opportunity to quantify reach-scale channel response in two reaches downstream of debris flow channels for which high-resolution pre-fire geomorphic data exist. We use repeat structure from motion (SfM) surveys in addition to surface-based bedload transport modeling to examine reach-scale changes in bed surface grain size, bedload transport capacity, and channel stability following the Dolan Fire. We also employ repeat airborne lidar surveys to contextualize reach-scale channel changes, and to understand how Big Creek accommodates and recovers from post-fire disturbance at the basin scale.

2. Study Site

The Big Creek watershed is a steep coastal basin encompassing 57 km^2 in the Santa Lucia Mountains along California's Big Sur coast (Figure 1a). The total relief in the Big Creek watershed is 1,500 m, and streams in the Big Creek watershed are steep, bouldery, jammed channels and are largely dominated by step-pool and cascade morphology (Church, 2006; Montgomery & Buffington, 1997). Prior to the wildfire, study reaches in Big Creek

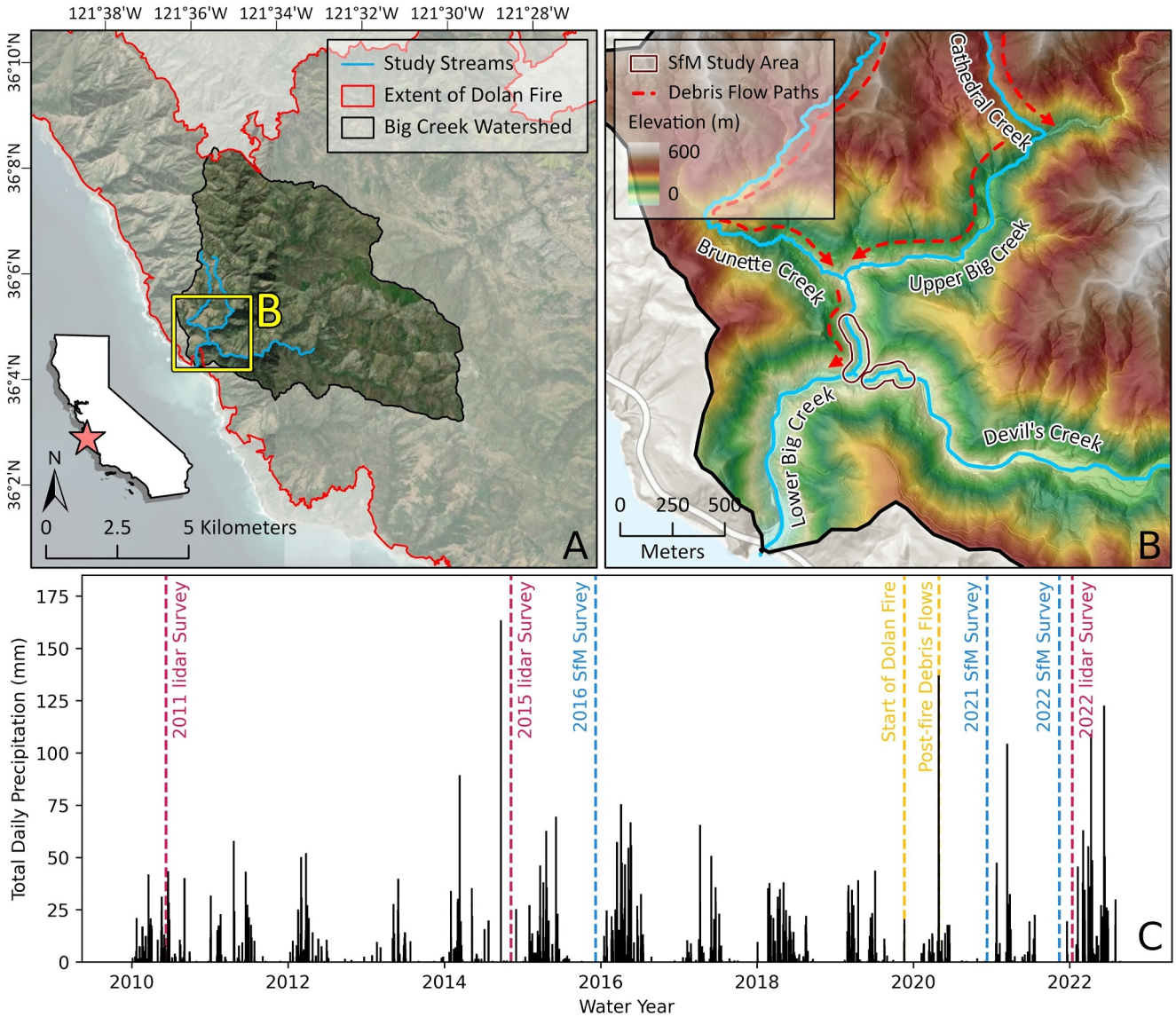

Figure 1. (a) Footprints of the Big Creek watershed and 2020 Dolan Fire along California's central coast. (b) Structure from motion study area within the Big Creek watershed. (c) Total daily precipitation at the Whale Point weather station within the Big Creek watershed. Dotted lines denote the dates of surveys, the onset of the Dolan Fire, and post-fire debris flows in Big Creek.

and Devil's Creek were cobble- and boulder-bedded with gradients of 6.8% and 5.2%, respectively. Upper hillslopes in the Big Creek watershed are partially rock-dominated with pockets of thin soil, whereas lower hillslopes are thinly soil-mantled. Bedrock geology in the Santa Lucia Mountains is complex and somewhat poorly constrained. The Big Creek watershed consists largely of Cretaceous magmatic and metamorphic rocks within the Salinian Block in the upper watershed. The middle and lower watersheds are characterized by Mesozoic granite, late Jurassic and Cretaceous metasedimentary rocks, and Cretaceous conglomerates (Dibblee Jr, 1974; Johnston et al., 2018).

Regional climate in Big Sur is characterized by dry summers and wet winters (Henson & Usner, 1996). Average yearly precipitation ranges from 1,000 mm along the coast to 2,000 mm at higher elevations within the Santa Lucia Mountains (Henson & Usner, 1996). Atmospheric rivers dominate regional precipitation, accounting for 30%–50% of total precipitation and 60%–100% of extreme precipitation along the U.S. West Coast (Dettinger, 2013; Dettinger et al., 2011; Eldardiry et al., 2019; Hecht & Cordeira, 2017; Li et al., 2022). Multi-year

droughts are also prevalent in coastal California, the two most recent of which lasted from 2012 to 2016, and from 2020 to 2022 (Griffin & Anchukaitis, 2014; Hoell et al., 2022).

Ecology in California's Central Coast Bioregion is highly elevation-dependent (Henson & Usner, 1996). In the Big Creek watershed, ridgelines and upper valley walls are dominated by chaparral ecosystems, which thrive in dry summers and wet winters (Tietje et al., 2019). Chaparral ridgelines and upper valley walls transition to mixed hardwood-conifer forests along lower valley walls and valley floors (Tietje et al., 2019). Notably, streams in the Big Creek watershed contain steelhead trout (*Oncorhynchus mykiss*; anadromous rainbow trout), for which spawning success is highly dependent on fluvial morphology (Everest & Meehan, 1981; Harrison et al., 2018; Kondolf & Wolman, 1993).

In August 2020, The Dolan Fire burned approximately 97% of the Big Creek watershed; the upper watershed experienced the most severe burns (Figure S5 in Supporting Information S1) (United States Forest Service, 2020). Following the fire, an atmospheric river event in January 2021 triggered post-wildfire debris flows in the Big Creek watershed; this atmospheric river event represents a 6-year rainfall event for the Big Creek watershed. Debris flows initiated in the headwaters of Brunette and Cathedral Creeks: small, steep tributaries of Big Creek with average gradients of 17.2% and 25.2% and Melton ratios of 0.64 and 0.53, respectively. Cathedral and Brunette Creek's confluences with Big Creek are 0.27 and 1.58 km upstream of our Big Creek focus reaches, respectively.

We focus our analyses on study reaches in Big Creek and Devil's Creek, a tributary to Big Creek which did not experience post-fire debris flows in 2021. Study reaches in Big Creek and Devil's Creek are step-pool dominated Strahler fourth-order channels that lie just upstream of their confluence (Figure 1). Big Creek and Devil's Creek have Melton numbers of 0.27 and 0.28, respectively, situating our study reaches just outside of the debris flow range (Jackson et al., 1987; Wilford et al., 2004). Our Big Creek study reach is tightly confined, has an average slope of 6.8%, and drains 27 km^2. Our Devil's Creek study reach has an average slope of 5.2%, drains 29 km^2, and is less confined than our Big Creek study reach. Big Creek and Devil's Creek share similar channel dimensions at high flow (Table S1 in Supporting Information S1); both streams were cobble- and boulder-dominated cascade and step pool channels with both wood- and boulder-enforced steps prior to post-fire disturbance. Contrasting post-fire conditions in Big Creek and Devil's Creek provide an opportunity for comparison between two otherwise similar streams in a burned watershed.

3. Methods

We combine reach-scale SfM data with hydraulic modeling, bedload transport modeling, and channel stability modeling to quantify post-fire changes in channel morphology and dynamics. SfM surveys cover a section of channel of approximately 230 m in length in both Big Creek and Devil's Creek. We then used basin-scale lidar change detection to identify spatial patterns of aggradation and incision, and to better understand the drivers of reach-scale geomorphic change following the Dolan fire.

3.1. Structure From Motion Photogrammetry and Field Observations

We conducted SfM surveys using a mast-mounted camera in Summer 2016 (pre-fire), 2021 (one year post-fire, six months after debris flows), and 2022 (two years post-fire, 18 months after debris flows) to characterize reach-scale geomorphic change following post-fire debris flows in the Big Creek watershed. We generated high-resolution orthoimages from SfM models using Agisoft Metashape, and co-registered 2016, 2021, and 2022 images to ensure consistency between measurements across timesteps. SfM surveys yielded high-resolution orthoimagery of Big Creek and Devil's Creek with pixel resolutions ranging from 1.0 to 1.9 mm (Figure 1b). To prepare pre- and post-fire SfM-derived orthoimages for grain size data collection, we outlined and masked the water surface and performed an object-based, supervised classification to delineate and mask vegetation out of each image (Figure 2). This classification produced user and producer accuracies greater than 90% for both information classes in every orthoimage and proved to be an effective method of isolating bed surface material for grain size characterization.

During 2016, 2021, and 2022 SfM surveys, we recorded field observations of channel morphology upstream, downstream, and within our SfM study reaches. We also present observations from SfM-derived orthoimages.

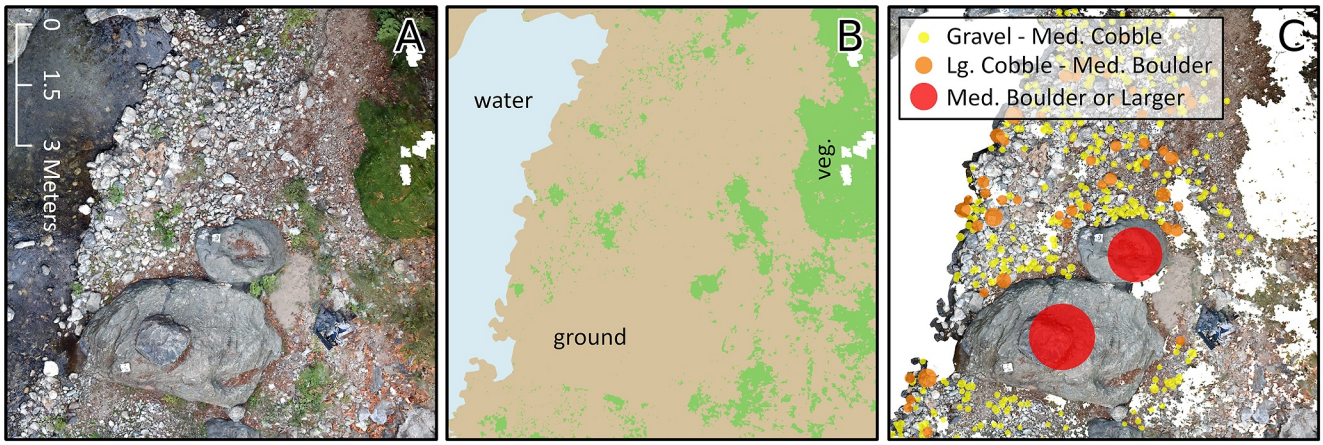

Figure 2. (a) Subset of one 2022 structure from motion orthoimage in Big Creek. (b) Classified orthoimage. (c) Processed orthoimage, with vegetation and water masked out, overlain with PebbleCounts (Purinton & Bookhagen, 2019) identified grains symbolized by b-axis diameter.

3.2. Bed Surface Grain Size Distribution

The bed surface grain size distribution in stream channels has important implications for sediment transport, channel stability, and aquatic habitat (Dietrich et al., 2005; Eaton et al., 2020; Harrison et al., 2018; Kondolf & Wolman, 1993; MacKenzie & Eaton, 2017; Riebe et al., 2014; Wilcock & Crowe, 2003). We use PebbleCounts (Purinton & Bookhagen, 2019), a python-based remote sensing tool, to characterize grain size distribution in pre- and post-fire orthoimagery. PebbleCounts uses a K-means segmentation algorithm, which clusters pixels that are similar in color and spatial location to identify and automatically measure grains in orthoimagery (Purinton and Bookhagen, 2019, 2021). PebbleCounts generates best-fit ellipses from manually selected segments, and measures ellipse diameter along and perpendicular to the longest axis (assumed to be a- and b-axis grain diameter, respectively), segment area, and ellipse area (Purinton & Bookhagen, 2019).

We use b-axis grain diameter and ellipse area outputs from PebbleCounts to generate area-weighted grain size distributions. In principle, this method resembles traditional field-based pebble count and grid count methods of quantifying surface grain size distribution, where the number of measured particles is determined by the number of grains that are successfully delineated by K-means segmentation (Bunte & Abt, 2001).

PebbleCounts provides a robust characterization of surface grain size distributions with several limitations. We note that grain size measurements only capture exposed portions of channel bars, but 2016, 2021, and 2022 SfM surveys took place during the lowest flows of the year with the highest possible bar exposure. Additionally, this method does not capture grains with segments that include fewer than 20 pixels. As such, our grain size distributions do not include grains with b-axis diameters smaller than approximately 0.025 m; there is minimal variation in this lower grain detection threshold across study reaches and timesteps. We note that this methodology biases our bed surface grain size distributions toward larger grain sizes. We use remotely sensed grain size distributions to model bedload transport capacity and channel stability under pre-fire, one year post-fire, and two years post-fire conditions in our SfM study reaches.

3.3. Hydraulic Modeling

Sediment transport capacity and channel stability models require estimates of bed shear stress. We assume steady uniform flow, calculating total bed shear stress (τ_o) as

$$\tau_o = \rho g R S \quad (1)$$

where R is the hydraulic radius (m), S is the channel slope, g is gravitational acceleration (9.81 m/s^2), and $\rangle$ is the density of water (997 kg/m^3). We estimate flow depth and slope over the full reach length, which is greater than the backwater length scale for these sites, making uniform flow a reasonable approximation (Paola & Mohrig, 1996). To calculate reach-average hydraulic radius for each of our study reaches, we use Manning's equation:

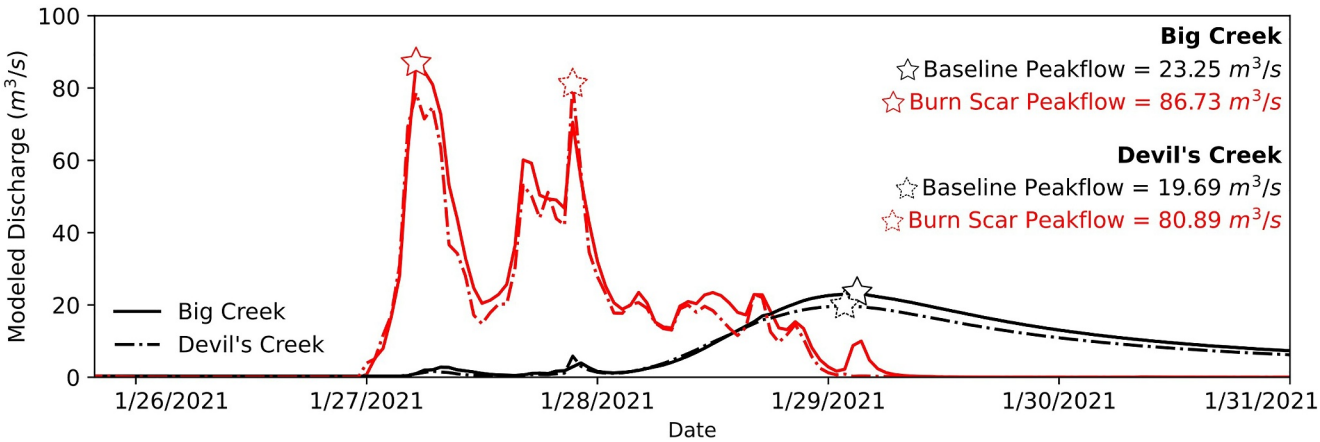

Figure 3. WRF-Hydro simulated baseline and burn scar incorporated hydrographs from Li et al. (2022) for Big Creek and Devil's Creek during the rainfall event from 26 January 2021 to 31 January 2021, which triggered post-fire debris flows in Big Creek. Stars denote peak flows.

$$u = \frac{R^{\frac{2}{3}} S^{\frac{1}{2}}}{n} \tag{2}$$

where u is the average downstream velocity (m/s), and n is roughness. Assuming a rectangular channel of reach-average flow depth h (m) and channel width w (m):

$$R = \frac{wh}{2h + w} \tag{3}$$

and

$$Q = whu \tag{4}$$

where Q is discharge in (m^3/s). We solve for h iteratively using Equations 1–3.

We estimate Manning's n for each of our sites using a gradient-based relationship from Jarrett (1984), which is explicitly focused on high gradient streams:

$$n = 0.39 S^{0.38} R^{0.16} \tag{5}$$

We estimate high flow channel widths using the 2016 and 2021 SfM orthoimages, dividing the full unvegetated channel area by the reach length. We used lidar DEMs to measure reach-average channel slope.

Due to a lack of field-based streamflow measurements in Big Creek and Devil's Creek, we used simulated peak flow values from Li et al. (2022) to estimate pre- and post-fire shear stress for bedload transport and channel stability calculations. Li et al. (2022) modified WRF-Hydro, a physics-based hydrologic model, to simulate streamflow in four burned watersheds in coastal California, including the Big Creek watershed. They presented streamflow simulations under both burn and non-burn scenarios for the rainfall event that triggered post-fire debris flows in Big Creek during January 26–29, 2021. We use burn-scar peak flows from Li et al. (2022) in our one- and two-year post-fire hydraulic models, and baseline non-burned peak flows in our pre-fire hydraulic model (Figure 3a). Hydrologic modeling from Li et al. (2022) produced discharges for 100 m grid cells at the outlets of Upper Big Creek and Devil's Creek. We rely on these model results for input discharge values alone, and perform the additional hydraulic calculations described above to inform sediment transport and channel stability modeling.

Unburned basins surrounding Big Creek record between a 1.5- to 5-year recurrence interval peak flow [based on historical data from the Big Sur River, Nacimiento Creek, and San Antonio River United States Geological

Survey (USGS) stream gages] for the 6-year recurrence interval rainfall event [based on historical data from the Whale Point Weather Station within the Big Creek watershed] which occurred between January 26th - 29th, 2021. Notably, we assume that discharges from the sensitivity experiment presented in Li et al. (2022) are reasonable estimates of flow under pre-fire and one year post-fire conditions, but maintaining constant discharge two years post fire likely introduces considerable error in bedload transport capacity and channel stability modeling (see Section 5.1 for further discussion). Li et al. (2022) also note that model results rely on potentially flawed meteorological data. To account for potential uncertainty related to meteorological inputs, we incorporate an uncertainty analysis for which we vary input discharge and flow width by 10% to present upper and lower bounds for bedload transport capacity and A_{stab}.

Immobile boulders and steps accommodate between 40% and 70% of the total boundary shear stress (τ_0) in step pool streams, reducing grain stress (τ'), or the shear stress available to transport mobile sediment on the channel bed (Canovaro et al., 2004; Church & Zimmermann, 2007; Yager et al., 2007, 2012; Zimmermann & Church, 2001). Implementing stress partitioning in the Big Creek study reaches using a robust approach such as that described by Yager et al. (2012) was not feasible in the scope of this study. Instead, we used observed grain size changes between 2021 and 2022 to calibrate the degree of stress partitioning in Big Creek. We find that a τ' value equal to $0.5\tau_0$ is capable of mobilizing grains up to 0.5 m, which grain size changes indicate were mobile between 2021 and 2022. This value is equivalent to the degree of stress partitioning observed in the Erlenbach by Yager et al. (2012), and falls within the range of values reported by Canovaro et al. (2004) for a stepped flume. We also incorporate potential uncertainty in shear stress partitioning into our analysis below. We present upper and lower bounds for bedload transport capacity and A_{stab}, for which we set grain stress (τ') equal to $0.6\tau_0$ and $0.4\tau_0$, respectively.

3.4. Bedload Transport Capacity and Channel Stability

Bedload transport capacity is largely a function of grain size and shear stress, both of which changed following post-fire debris flows in Big Creek. We modify the Wilcock and Crowe (2003) equations to estimate bedload transport capacity as a function of grain size (D), grain stress (τ'), and critical (or reference) Shields stress (τ_{ri}). We used PebbleCounts-generated bed surface grain size distributions and reach-average, partitioned bed shear stresses and flow widths to calculate the volumetric bedload transport capacity for the Big Creek and Devil's Creek study reaches. We opt to use this modeling approach over other approaches calibrated for steep channels (e.g., Recking, 2013) to capture changes in bedload transport capacity across the entirety of the bed surface grain size distribution.

Wilcock and Crowe (2003) describes dimensionless transport rate (W_i^*) for each size class (i) as a function of the ratio between grain shear stress and the reference shear stress for each size class:

$$W_i^* = \begin{cases} 0.002\phi^{7.5} \\ 14\left(1 - \dfrac{0.894}{\phi^{0.5}}\right)^{4.5} \end{cases} \tag{6}$$

where:

$$\phi = \frac{\tau'}{\tau_{ri}} \tag{7}$$

We estimate reference Shields stress as a function of channel slope using an empirical relationship established in Prancevic and Lamb (2015):

$$\tau_{r50}^* = 0.395^{0.44} \tag{8}$$

To account for grain hiding effects, we employ a hiding function to calculate reference shear stress for a given grain size fraction (τ_{ri}):

$$\frac{\tau'_{ri}}{\tau_{r50}} = \left(\frac{D_i}{D_{50}}\right)^b \quad (9)$$

Wilcock and Crowe (2003) provide a function to define the hiding exponent (b) that is likely inadequate for steep channels. Previous work suggests that the effect of hiding is reduced in steep streams (Mao et al., 2008; Scheingross et al., 2013; Yager et al., 2012). These studies modify the hiding exponent in empirical bedload transport relationships from Parker (1990) to more accurately predict bedload transport in steep streams; we implement a similar approach using the empirical bedload transport relationships from Wilcock and Crowe (2003). We chose to adopt the hiding exponent from Scheingross et al. (2013) ($b = 0.49$) as their study calibrates the hiding exponent for multiple streams with similar slope and morphology to Big Creek and Devil's Creek.

Channel stability for a given discharge is dependent on the mobility of bed surface sediment. If the surface grain size distribution in channels throughout the Big Creek watershed changed following the Dolan Fire, channel stability likely evolved in tandem with grain size. A_{stab} is a metric for channel stability, which refers to the proportion of the channel bed that is immobile at a given shear stress (Eaton et al., 2020). A_{stab} is predicated on the idea that a subset of immobile grains can maintain channel stability even when the dimensionless shear stress associated with D_{50} exceeds the threshold for motion (Eaton et al., 2020). Channel stability thresholds for this metric are calibrated for streams with riffle-pool morphology, but we use A_{stab} as a concise metric to quantify the joint effects of grain size and hydrologic change on the post-debris flow sediment transport conditions in Big Creek.

A_{stab} is equal to the sum of the fraction of each size class that is immobile under a given shear stress (Equation 10, Equation 11).

$$A_{stab} = \Sigma I_i F_i \quad (10)$$

where:

$$I_i = 1 - \left(\frac{1}{1 + exp\left(-4.3\left(\frac{\tau}{\tau_{ri}} - 1.5\right)\right)}\right) \quad (11)$$

We used grain size distributions from 2016, 2021, and 2022, critical Shields stress, and reach-average bed shear stress from HEC-RAS flow modeling to calculate A_{stab} in Big Creek and Devil's Creek in 2016, 2021, and 2022.

Our modeling relies on a variety of assumptions necessitated by data set limitations. As such, we vary hydraulic parameters to present upper and lower bounds for bedload transport capacity and A_{stab} results. We emphasize that our results are subject to a high degree of uncertainty and choose to focus our interpretations of model results on relative relationships through time rather than specific values reported herein.

3.5. Lidar Differencing

Prior to the Dolan Fire, airborne lidar data sets for Big Creek and Devil's Creek were collected in 2011 and 2015 (OpenTopography, 2013, 2016). In 2022, a post-fire airborne lidar data set was collected, encompassing Big Creek, Devil's Creek, Cathedral Creek, and Brunette Creek (OpenTopography, 2023). 2011 and 2015 lidar surveys yielded vertical accuracies of 0.20 and 0.15 m, respectively, and point densities of 11.66 points/m^2. The 2022 lidar survey yielded a vertical accuracy of 0.10 m and a point density of 84.65 points/m^2. All lidar data sets were processed to generate 1 m-resolution digital terrain models (DTMs) (OpenTopography, 2013, 2017, 2022).

We used digital elevation model (DEM) differencing to identify zones of significant geomorphic change in Big Creek, Devil's Creek, Cathedral Creek, and Brunette Creek. Before conducting differencing, we co-registered lidar point clouds using an iterative closest point algorithm (CloudCompare (version 2.13), 2023). We used Geomorphic Change Detection (GCD) Software (Bailey et al., 2020) to generate a DEM of difference (DoD) between 2011 and 2022 lidar-generated, co-registered digital terrain models, and sum 1 m^2 DoD grid cells to

approximate volumetric change. We chose to perform primary differencing analyses using 2011 and 2022 lidar products because the 2015 lidar data set contains numerous problematic artifacts within the channel. Further, the 2015 lidar data set does not capture Cathedral Creek and Brunette Creek where post-fire debris flows initiated. Differencing between 2011 and 2015 lidar data sets suggests very minimal channel change between 2011 and 2015 (Figure S4 in Supporting Information S1).

We used GCD's probabilistic thresholding functionality to capture topographic changes that exceeded a 99% probability threshold, which yielded a minimum level of detection of ±0.57 m (Bailey et al., 2020). We restricted DTM differencing analyses to valley floors in Big Creek, Devil's Creek, Cathedral Creek, and Brunette Creek; steep valley walls in the Big Creek watershed exacerbate any co-registration error between lidar data sets and are thus more likely to produce inaccurate DoD values. As such, the DTM differencing analyses presented here does not capture hillslope contributions. Notably, our analysis does not account for material that was deposited in Cathedral and Brunette Creek between the onset of the Dolan Fire and post-fire debris flows. This through-flowing sediment load likely accounts for a considerable portion of total post-fire sediment yield; following the Dolan Fire, dry ravel likely loaded Cathedral and Brunette Creek, priming channels for post-fire debris flows (DiBiase & Lamb, 2020). Further, our analysis also fails to quantify post-fire sediment contributions from Big Creek upstream of its confluence with Cathedral Creek. We validate the results of DTM differencing using field photos and observations from 2016, 2021, and 2022 field campaigns.

4. Results

4.1. Field Observations

Throughout Upper Big Creek, we observed extensive deposition of poorly sorted sediment up to 1 m above the 2021 channel bed, composed of sand to large boulders following post-fire debris flows. The composition of debris flow-related sediment indicates that our Upper Big Creek study reached likely experienced debris floods, which may have occurred via dilution of upstream debris flows (Church & Jakob, 2020; Olsen, 2023). Debris flood sediment appears to have filled the channel, replacing formerly bouldery, vegetated banks with large swaths of sand, gravel and cobbles (Figure 4a). Debris floods also removed a major log jam in Upper Big Creek that was emplaced before 2016 and incised into the wedge of sediment upstream of the log jam. Immediately downstream of Big Creek's confluence with Brunette Creek, post-fire debris flows emplaced a valley-wide log jam, approximately 6 m tall and 35 m wide. Upstream of the log jam, we observed a valley-spanning, boulder-rich wedge of sediment behind the log jam. Downstream of the log jam, large wood was mostly absent in our SfM study reaches in Big Creek immediately following 2021 post-fire debris flows. Several large, deep pools in Big Creek surveyed in 2016 no longer existed in 2021. Bed sediment in Big Creek became finer and less uniform following post-fire debris flows (Figure 4a). Additionally, multiple large boulders that were present in 2016 were no longer present in 2021, and several new boulders were deposited and/or exhumed throughout Big Creek. By 2022, riparian species had re-colonized channel margins and mid-channel bars throughout Big Creek and gravel patches, while still more abundant than in 2016, became coarser and more uniform in grain size. In Big Creek, much of the sand that was deposited during 2021 debris flows was evacuated between 2021 and 2022 surveys (Figure 4a).

Notably, Devil's Creek exhibits little evidence of major geomorphic change. Pools, boulders, large wood, and dense riparian vegetation were prevalent prior to and following the Dolan Fire (Figure 4b). Discrepancies in post-fire geomorphic response between Big Creek and Devil's Creek likely stem from differences in connectivity and burn severity between the two sub-basins. Big Creek is incised into a narrow, tightly confined canyon, in which steep valley walls often serve as channel margins. Devil's Creek sits in a much broader valley, with similarly steep valley walls that are often up to 30 m away from the channel itself. As such, a typical reach in Big Creek exhibits greater connectivity to hillslope sediment sources than a typical reach in Devil's Creek, and fire-related sediment is less likely to reach Devil's Creek itself. Moreover, the Devil's Creek sub-basin burned less severely than the Upper Big Creek sub-basin (Figure S5 in Supporting Information S1).

4.2. Bed Surface Grain Size Distribution

Post-fire debris flows spurred changes in the bed surface grain size distribution in Big Creek. Upstream debris flows introduced additional fine sediment to our Big Creek study reach, reducing D_{16} and D_{50} from 0.34 to 0.11 m and 0.76 to 0.49 m, respectively, from 2016 to 2021 (Figure 5a). From 2021 to 2022, the bed surface grain size

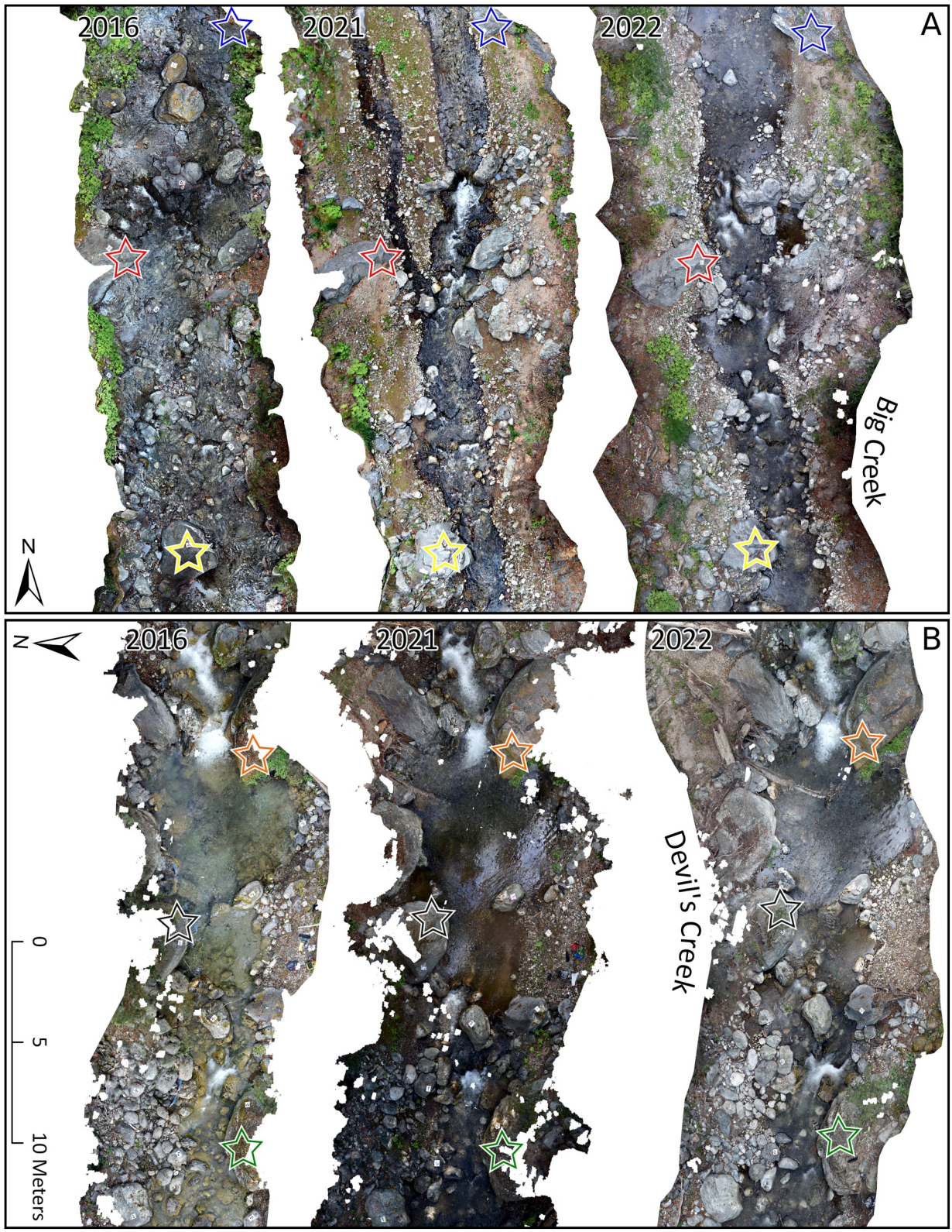

Figure 4. Subsets of structure from motion orthoimages from 2016, 2021, and 2022 surveys in (a) Big Creek, and (b) Devil's Creek. Stars denote landmarks between 2016, 2021, and 2022 orthoimages.

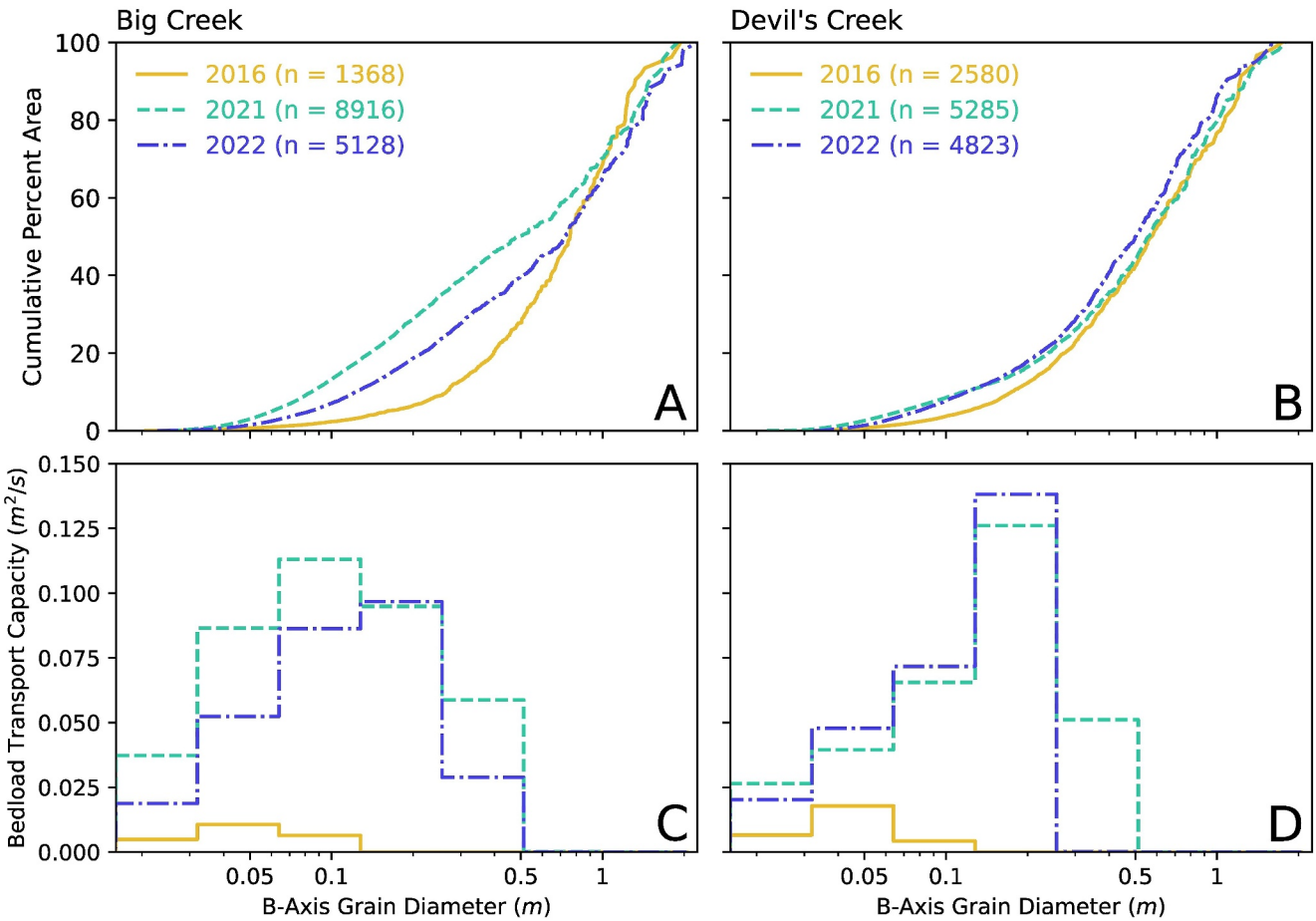

Figure 5. (a) Remotely sensed bed surface grain size distributions from 2016, 2021, and 2022 structure from motion (SfM) surveys in Big Creek. (b) Remotely sensed bed surface grain size distributions from 2016, 2021, and 2022 SfM surveys in Devil's Creek. (c) Modeled bedload transport capacity per unit-width for grain size bins in Big Creek. (d) Bedload transport capacity per unit-width for grain size bins in Devil's Creek.

distribution in Big Creek partially re-coarsened; D_{16} increased to 0.17 m, while D_{50} increased to 0.73 m (Figure 5a). D_{84} exhibited comparatively little change across all timesteps (Figure 5a). Like Big Creek, changes in Devil's Creek's grain size distribution are most apparent in the finer half of the grain size distribution, though the magnitude of change is far smaller. D_{16} became marginally finer in all Devil's Creek between 2016 and 2021. D_{50} and D_{84} exhibited no systematic change across study reaches in Devil's Creek from 2016 to 2021 (Figure 5b). From 2021 to 2022, D_{16} remained constant across all study reaches, while D_{50} became marginally finer. Average D_{84} did not exhibit systematic change across all three study reaches in Devil's Creek (Figure 5b).

4.3. Hydraulic Modeling

Hydraulic modeling yielded reach-average grain stresses of 430 and 253 Pa and average flow widths of 8.0 and 8.7 m in Big Creek and Devil's Creek, respectively (Figures 6a and 6b). One year post-fire, increases in peak flow discharges precipitate substantial increases in modeled reach-average shear stresses and flow widths in both Devil's Creek and Big Creek (Figures 6a and 6b).

4.4. Bedload Transport Capacity and Channel Stability

Post-fire changes in bedload transport capacity and channel stability reflect post-fire changes in surface grain size distribution, channel geometry, roughness, and basin hydrology. Big Creek's bedload transport capacity response to post-fire debris flows is characterized by increases immediately following disturbance, followed by a partial recovery toward pre-fire conditions two years post-fire. We note that any changes in bedload transport capacity and A_{stab} from one to two years post-fire stem from changes in the bed surface grain size distribution and

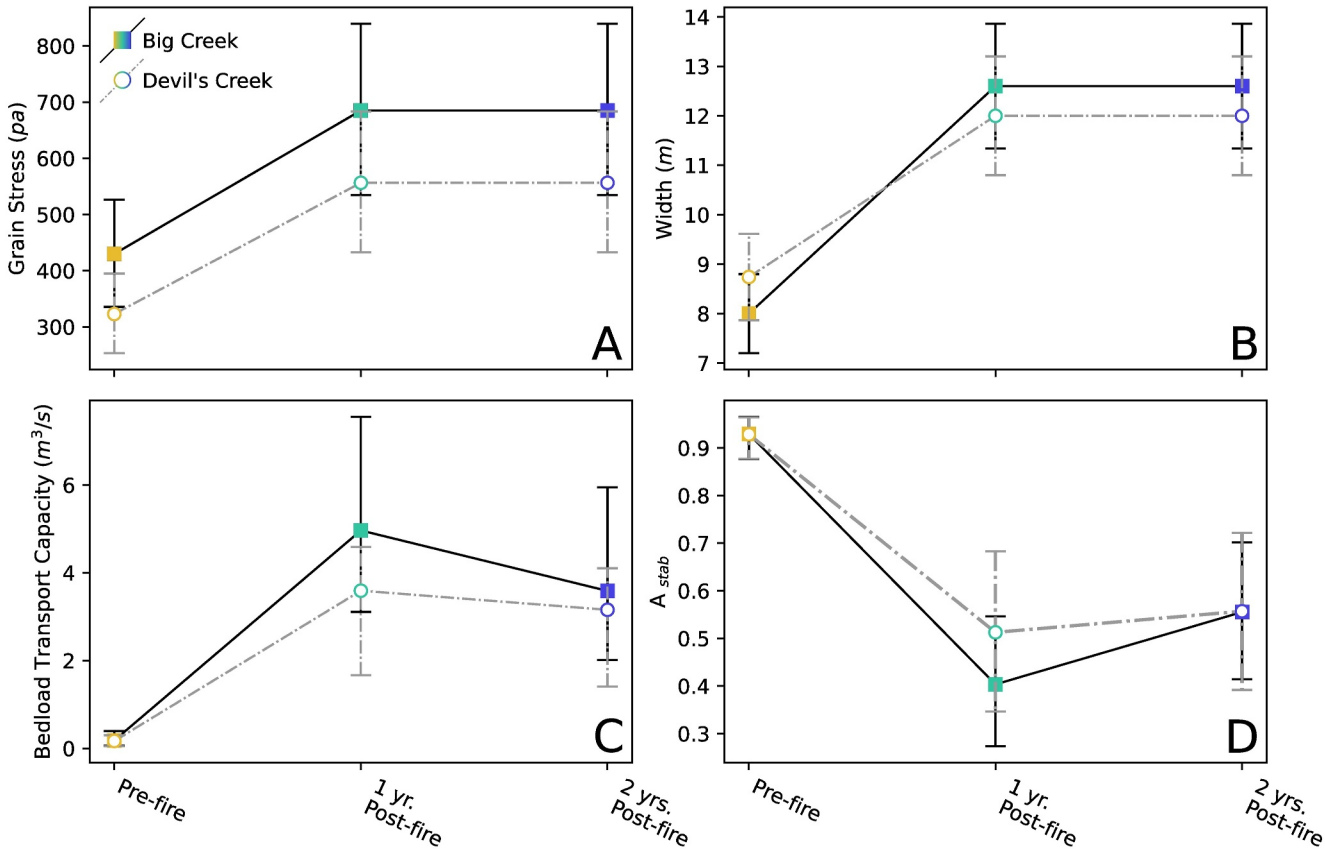

Figure 6. (a) Reach-average shear stresses (b) flow widths, (c) volumetric bedload transport capacity, and (d) A_{stab} under pre-fire, one year post-fire, and two years post-fire conditions in Big Creek and Devil's Creek.

hydraulic roughness, as other model inputs (discharge, channel geometry) remain constant. Post-fire changes in both the bed surface grain size distribution and basin hydrology contribute to changes in bedload transport capacity and channel stability. We discuss the respective roles of each variable in Section 5.1.

Modeled bedload transport capacity in Big Creek increased 28-fold one year post-fire, from 0.18 m^3/s to 5.0 m^3/s, coinciding with an increase in modeled bedload grain size (Figures 5c and 6a). From one year post-fire to two years post-fire, modeled bedload transport capacity decreased in Big Creek, while the grain size distribution of the modeled sediment load became coarser (Figures 5c and 6a). Changes in channel stability mirror changes in bedload transport capacity (Figure 6b). One year post-fire, A_{stab} decreased from 0.93 to 0.40 in Big Creek. Two years post-fire, A_{stab} in Big Creek increased to 0.56 (Figures 5c and 6b). Notably, even lower bound estimates for A_{stab} indicate that the largest 27% of grains in Big Creek remained stable one year post-fire.

Devil's Creek also exhibited initial post-fire increases in modeled bedload transport capacity. Both the volume and grain size of the modeled sediment load increased substantially one year post-fire, and decreased marginally two years post-fire. Like Big Creek, study reaches in Devil's Creek were exceptionally stable prior to the Dolan Fire. Modeled A_{stab} decreased across in Devil's Creek from 0.93 to 0.51 one year post-fire and increased to 0.55 two years post-fire (Figures 5d and 6b).

4.5. Lidar Differencing

Topographic differencing between 2011 and 2022 data sets records substantial systematic topographic change throughout the Big Creek watershed. Both Cathedral and Brunette Creek are widely dominated by scour, with large failures visible in multiple locations down the length of both channels. Cathedral and Brunette Creek exhibit approximately 23,000 and 9,000 m^3 of scour between 2011 and 2022, respectively (Figure 7 and Figure S1 in Supporting Information S1).

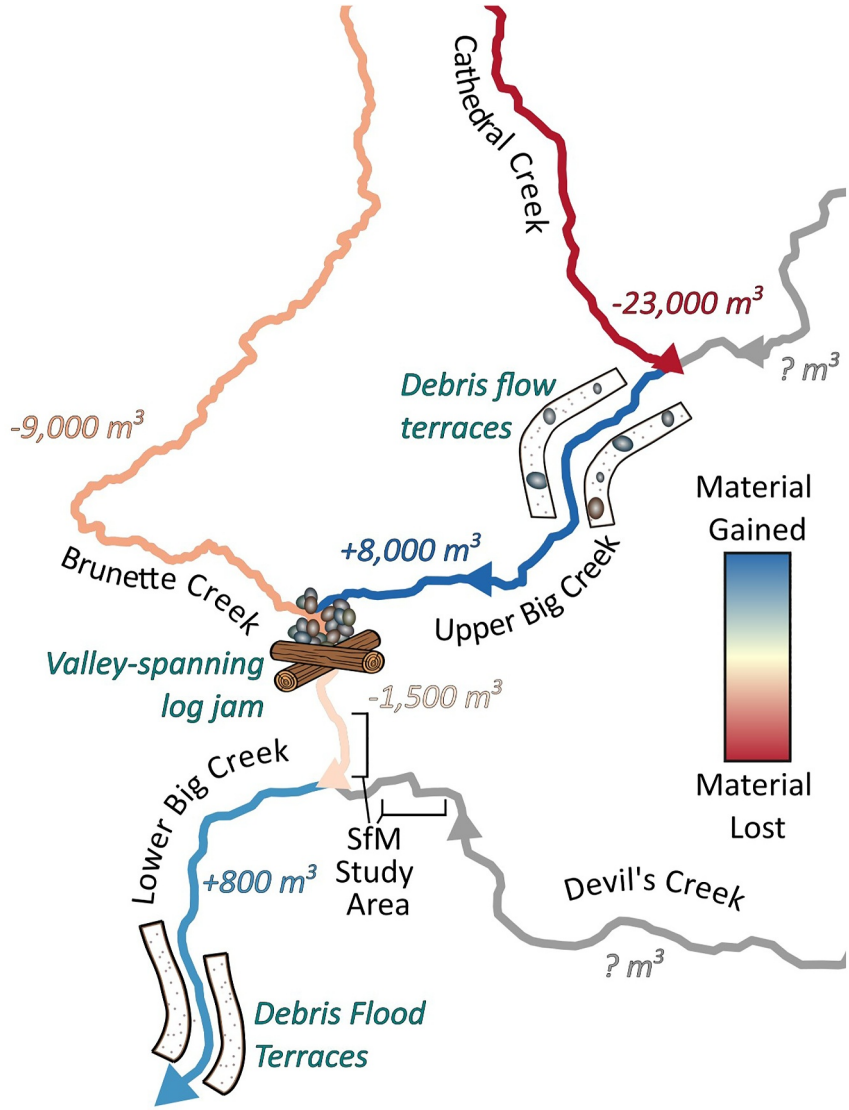

Figure 7. Simplified schematic of post-fire sediment contributions and storage for streams in the Big Creek watershed.

Upstream of its confluence with Brunette Creek, Big Creek experienced extensive deposition (Figure S2 in Supporting Information S1). The most notable depositional feature in Big Creek is located behind the valley-spanning log jam at Big Creek's confluence with Brunette Creek (Figure 8). Cumulatively, 3,300 m^3 of material was deposited behind the log jam between 2011 and 2022, with a maximum observed elevation increase of 5 m. Accumulation behind this log jam accounts for 10% of the total material exported from Cathedral and Brunette Creek, and 37% of the total material deposited upstream of Big Creek's confluence with Brunette Creek. Between confluences with Brunette Creek and Devil's Creek, Big Creek is largely dominated by incision (Figure 7). The most notable erosional feature lies 200 m downstream of the confluence with Brunette Creek, where debris flows removed a large log jam emplaced prior to 2016 and incised into alluvium built up behind the log jam (Figure 8). Under the assumption that scour volumes in Cathedral and Brunette Creek reasonably approximate post-fire debris flow volume, 72% (or approximately 23,000 m^3) of post-fire debris flow material sourced from Cathedral and Brunette had exited the fluvial system by 2022 (Figure 7). Substantial beach growth at the mouth of Big Creek provides some anecdotal support for this finding. Notably, several major hotspots of geomorphic change in Big Creek between 2011 and 2022 coincide with locations of newly created and destroyed log jams within the channel (Figure 8).

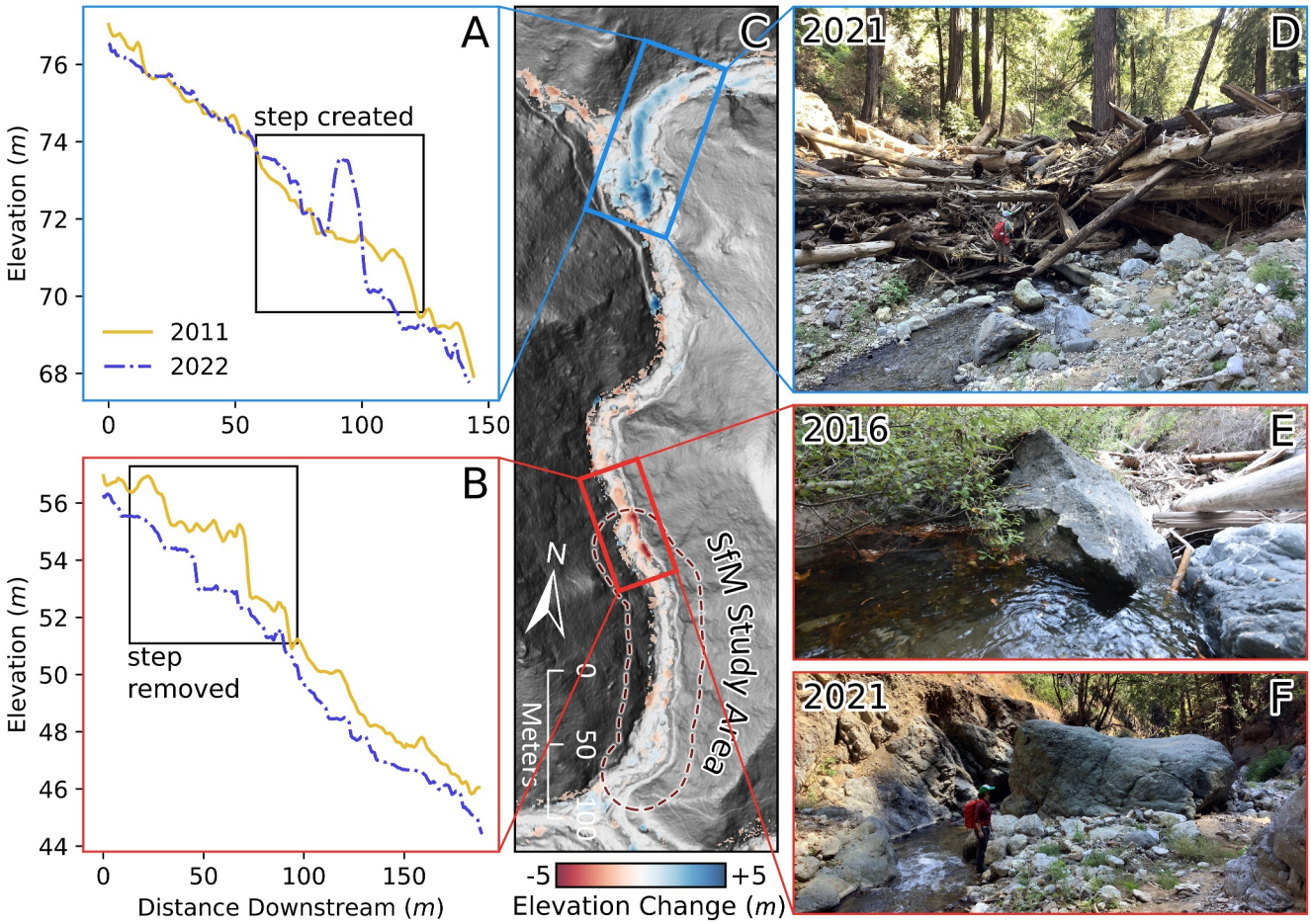

Figure 8. (a), (b) Longitudinal profiles extracted from 2011 to 2022 lidar DTMs. (c) DEM of difference from 2011 to 2022 for Big Creek between confluences with Brunette Creek and Devil's Creek. (d) 2021 field photo of the newly constructed valley-spanning log jam in Big Creek just downstream of the Brunette Creek confluence. (e) 2016, and (f) 2021 field photos of the location of a large log jam which was destroyed during 2021 post-fire debris flows.

Topographic differencing in Devil's Creek reveals sporadic topographic change from 2011 to 2022 (Figure S3 in Supporting Information S1). The most prominent depositional features in Devil's Creek exist along channel margins near the outlets of small drainages. Cumulatively, the lower 5 km of Devil's Creek gained approximately 440 m^3 of material between 2011 and 2022 within the channel. In general, Devil's Creek did not appear to have experienced widespread systematic aggradation or incision in response to the Dolan Fire during our study period.

5. Discussion

5.1. Controls on Post-Fire Bedload Transport Capacity

Post-fire changes in bedload transport capacity and channel stability in our SfM study reaches in Big Creek and Devil's Creek stem from changes in the bed surface grain size distribution and grain stress. Changes in grain stress in Big Creek and Devil's Creek largely stem from changes in input discharge. To evaluate the respective influence of fire-related changes in discharge and bed surface grain size distribution, we conducted a simple sensitivity analysis, comparing our best approximations of bedload transport capacity to scenarios in which each variable remains constant at pre-fire conditions, while the others evolve over time.

In Big Creek, post-fire discharge increases and bed surface grain size fining account for roughly equivalent proportions of the increase in bedload transport capacity one year post-fire, while bed surface coarsening alone accounts for the decrease in bedload transport capacity two years post-fire. However, we note that our bedload transport capacity calculations do not account for post-fire hydrologic recovery, which would impel further decreases in bedload transport capacity two years post-fire (Figures 9a and 9c). We also note that modest changes in

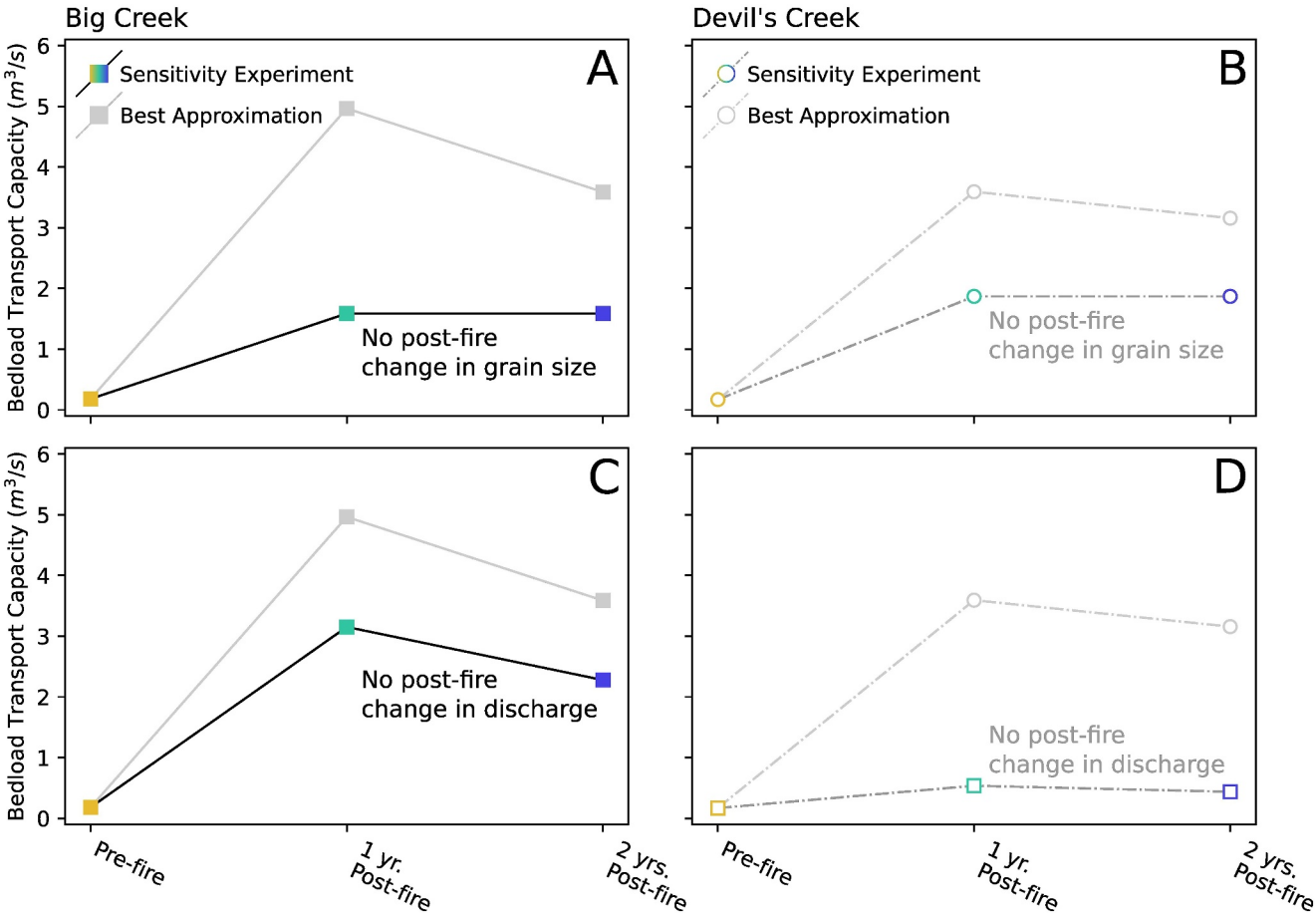

Figure 9. Modeled bedload transport capacity under pre-fire, one year post-fire, and two years post-fire conditions. Gray lines and markers represent our best approximation of bedload transport capacity in which each variable evolves, while lines with colored markers represent bedload transport capacity approximations with (a) no post-fire change in grain size in Big Creek, (b) no post-fire change in grain size in Devil's Creek, (c) no post-fire change in discharge in Big Creek, and (d) no post-fire change in discharge in Devil's Creek.

channel geometry following post-fire debris flows have little impact on bedload transport capacity (Olsen, 2023). In Devil's Creek, post-fire increases in discharge account for most of the modeled bedload transport capacity increase one year post fire, while marginal fining accounts for minor increases in bedload transport capacity (Figures 9b and 9d).

Importantly, studies from other sites suggest that the hydrologic impact of wildfire subsides over time, with some watersheds exhibiting 95% recovery within 7 years (Wagenbrenner et al., 2021). Timescales of post-fire hydrologic recovery are dependent on several variables, including post-fire precipitation patterns, aspect, and burn severity (Kinoshita & Hogue, 2011). Following the 2009 Station Fire in Southern California, hillslopes in the Arroyo Seco watershed (approximately 350 km southeast of Big Creek, and of similar size to the Big Creek watershed) exhibited substantial decreases in modeled saturated hydraulic conductivity within one year after the fire, followed by persistent increases toward pre-fire conditions for 5 years post-fire, at which point modeled saturated hydraulic conductivity had returned to pre-fire conditions (Liu et al., 2021). Burn scar modeled discharges for Big Creek and Devil's Creek reflect hydrologic conditions immediately after the Dolan Fire. Thus, WRF-Hydro simulated hydrographs for Big Creek and Devil's Creek likely represent reasonable peak flows for one year after the Dolan Fire. By two years after the Dolan Fire, however, hydrologic conditions had potentially recovered considerably. Realistically, post-fire hydrologic conditions two years post-fire exist between baseline and burn scar discharge values used here, and thus we likely overestimate bedload transport capacity two years post-fire.

5.2. Timescales of Sediment Delivery and Geomorphic Recovery

SfM study reaches in Big Creek experienced rapid geomorphic recovery following post-fire debris flows. Within two years after the Dolan Fire, D_{16} and D_{50} had re-coarsened substantially across all study reaches in Big Creek; by 2022, average D_{50} had coarsened to 95% of the pre-fire D_{50}. Further, results from lidar differencing in Big Creek, Cathedral Creek, and Brunette Creek indicate that, by volume, 72% of post-fire sediment scoured from colluvial hollows in which debris flows initiated had exited the watershed by 2022. An overwhelming majority of the remaining debris flow material in the watershed resides upstream of the log jam at the Brunette Creek confluence.

Downstream of this log jam, rapid recovery toward pre-fire conditions has continued since 2022 SfM and lidar surveys. In January 2023, a bomb cyclone event triggered widespread flooding across California. The USGS stream gage near the outlet of the Carmel River, approximately 50 km north of Big Creek, recorded a 10-year recurrence interval flood. Qualitative field observations following the 2023 flood event indicate further coarsening of the bed surface grain size distribution in our SfM study reaches and downstream. While Big Creek exhibits substantial geomorphic recovery downstream of the wood jam at the Brunette Creek confluence, the area just upstream of the wood jam has experienced continued aggradation during 2023 floods.

Recent studies of dam removals (scheduled events with ample opportunity to collect pre-event baseline data sets) may serve as a comparison point for our findings in Big Creek. In general, rivers are quite resilient to sediment pulses from dam removals, typically regaining stability within several years (East et al., 2023; Major et al., 2017). Recovery timescales for dam removal are similar to recovery timescales in Big Creek. However, whereas dam removals are engineered to mitigate catastrophic downstream response, no such mitigation measures exist in Big Creek.

The rate at which channels recover from episodic sediment supply perturbations depends on the rate at which excess sediment is evacuated from the fluvial system (Gran & Montgomery, 2005). In Big Creek, the Brunette Creek log jam serves to trap large volumes of sediment from Cathedral Creek, effectively cutting off upstream sediment supply to our SfM study reaches in Big Creek. This, in conjunction with elevated bedload transport capacities from post-fire changes in bed surface grain size and basin hydrology, spurs rapid evacuation of fire-related fine sediment and coarsening of the bed surface grain size distribution in Big Creek downstream of the Brunette Creek confluence. Importantly, although our results provide some insight into the rate of post-fire recovery in Big Creek, our analyses lack hydrologic time series data beyond 2021 and survey data beyond 2022, and thus do not capture the timescales of full post-fire geomorphic recovery.

Our lidar differencing results may offer further insight into the processes that govern long-term landscape evolution in Big Sur. Young and Hilley (2018) provided cosmogenic nuclide-derived basin-averaged erosion rates for 18 catchments in the Santa Lucia Mountains, including an erosion rate of 207.06×10^{-3} mm/yr for the Big Creek watershed. The Cathedral and Brunette Creek catchments encompass 1.55 and 2.59 km^2, respectively. Channels in these basins exported approximately 32,000 m^3 of material during 2021 debris flows, which equates to a basin-averaged erosion rate of 7.72 mm, or approximately 37 years-worth of erosion. This result, coupled with potentially frequent fire-recurrence in the California Central Coast bioregion, speaks to the importance of debris flows in the long-term landscape evolution of the Santa Lucia Mountains.

5.3. Channel Stability, Steps, and the Role of Wood

Large wood within stream channels accounts for substantial sediment storage; in particular, log jams may store disproportionately large volumes of post-fire sediment (Rengers et al., 2023; Short et al., 2015). Lidar differencing in Big Creek reveals that many hotspots of geomorphic change during post-fire debris flows occurred where debris flows destroyed or created log jams. The creation and destruction of these log jams introduce additional sediment supply perturbations beyond excess sediment delivery from post-fire debris flows. The strength and longevity of log jams are partially dependent on log diameter (Ennos & van Casteren, 2009; Rengers et al., 2023), and thus these debris flow-related log jams may be especially important in modulating long-term post-fire sediment supply for streams in the California central coast bioregion. Large Coast Redwoods often account for a considerable portion of the wood supply in the region (and largely comprise the log jam at the Brunette Creek confluence), while chaparral hillslopes and ridgelines prevalent throughout Big Sur are prone to frequent, intense burns (Figure S6 in Supporting Information S1). Thus, geomorphic response to wildfire in this

environment may be unique in comparison to surrounding bioregions to the north, which lack chaparral, and to surrounding bioregions to the south, which lack large wood supply (Figure S7 in Supporting Information S1).

Large wood and boulders control channel structure in step pool streams such as Big Creek (Hassan et al., 2023; Keller et al., 2015). Post-fire debris flows in Big Creek mobilized large boulders and both introduced and removed wood into and from the channel, and thus were capable of reconfiguring channel morphology. Our analysis suggests that clearwater floods alone are not capable of restructuring the channel. In Big Creek, even under burn scar hydrologic conditions and after considerable bed surface fining, clearwater floods are insufficient to mobilize the coarsest 25% of the grain size distribution, let alone these largest keystones which make up steps (Figures 5 and 6).

Topographic differencing analyses further support the long-term pre-fire stability in Big Creek, and the channel restructuring capabilities of post-fire debris flows. Topographic differencing between 2011 and 2015 lidar data sets indicates scattered, minor topographic change in Big Creek between 2011 and 2015. During this period, the channel structure remained widely unchanged. In contrast, topographic differencing between 2011 and the post-fire 2022 lidar data set showcases sweeping geomorphic change and major adjustments to channel morphology in Big Creek, where several existing steps were destroyed, and new valley-wide steps were created (Figure 8). Low-frequency, high-magnitude events are required to enact large-scale changes to channel structure in step pool streams (Chin & Wohl, 2005; Hassan et al., 2023; Lenzi et al., 2006). Our results indicate that debris flow events are critical in overhauling channel morphology in steep, bouldery, step pool streams such as Big Creek. In Big Creek, clearwater floods cannot generate the requisite force to restructure the channel, and thus elevated sediment transport rates and instability caused by grain size fining and post-fire discharge increases may be limited to mobile patches within an otherwise stable channel. These clearwater floods are thus inconsequential for large-scale channel dynamics. However, regardless of implications for channel morphology, post-fire bed surface instability and elevated sediment transport rates likely have implications for aquatic habitat in Big Creek.

5.4. Ecological Implications

Post-fire geomorphic change in Big Creek has a myriad of potential implications for aquatic ecosystems and salmonid spawning habitats. Quantifying the ecological impacts of post-fire debris flows is beyond the scope of our work, but these quantitative geomorphic data provide the basis for simple hypotheses about steelhead trout response in this well-studied basin.

Post-fire debris flows had immediate adverse effects on salmonids in Big Creek, as debris flows took place during winter, when steelhead trout typically return to freshwater habitats, and thus removed any fish in the channel. Following post-fire debris flows, Big Creek was largely inundated with fine sediment; excess fine sedimentation has adverse effects on the spawning habitat. Elevated fine sediment loads in riverine ecosystems may smother salmonid spawning substrate and limit primary production, which reduces available food sources for salmonids (Kemp et al., 2011). The months following post-fire debris flows in Big Creek coincide with the steelhead trout spawning season, and thus the salmonid population in Big Creek likely suffered from a year of inhibited production due to post-fire geomorphic disturbance. Furthermore, fining of the bed surface grain size distribution in Big Creek and post-fire changes in basin hydrology are responsible for channel instability and elevated bedload transport capacities. Elevated bedload transport capacities and channel instability leave potential salmonid spawning gravels vulnerable to scour, further reducing the areal percentage of the bed that is suitable for spawning. Additionally, several step-pools throughout Big Creek were buried during post-fire debris flows, eliminating resting habitat for salmonids and reducing habitat diversity as a whole (Everest & Meehan, 1981). Over longer timescales, however, salmonids will likely benefit from the introduction of new, suitably sized spawning gravels into formerly bouldery, marginal spawning habitats in Big Creek.

Notably, the presence of nearby Devil's Creek significantly improves recovery prospects for salmonids in the Big Creek watershed. Devil's Creek experienced far less geomorphic change than Big Creek, and thus serves as a stable refuge habitat for salmonids in the Big Creek watershed. Fish can spend Big Creek's dynamic geomorphic recovery period in Devil's Creek, and eventually return to what was once a marginal spawning habitat in Big Creek, now refreshed with suitable spawning substrate. Ongoing steelhead trout surveys in Big Creek and Devil's Creek will provide further insight into the fish population response to post-fire disturbance in the Big Creek watershed.

6. Conclusions

This study characterizes the geomorphic response to post-fire debris flows in the Big Creek watershed, a steep basin along California's Central Coast. Following post-fire debris flows in Big Creek, we observed substantial fining of the D_{16} and D_{50} in our Big Creek SfM study reaches. D_{84} remained largely unchanged after the fire, despite a wholesale overhaul of channel structure. Two years after wildfire, the bed surface grain size distribution in our SfM study reaches has re-coarsened substantially, which indicates rapid recovery toward pre-fire conditions. Post-fire changes to grain size distribution, coupled with changes in basin hydrology contribute to considerable change in bedload transport capacity in our Big Creek SfM study reaches. Comparatively, Devil's Creek exhibits minimal post-fire change in both bed surface grain size distribution and channel structure despite post-fire changes in basin hydrology, which spur increases in bedload transport capacity one year post-fire.

Debris flows are required to change channel structure in Big Creek via their capacity to transport both boulders and wood, which govern channel morphology and step-pool configuration in the channel. Even during elevated post-fire peak flows during a 6-year recurrence interval rain event, the boulders that control the step pool configuration in Big Creek remain immobile. Thus, step pool and cascade features in the channel likely remain static between debris flow events. Valley-spanning wood jams were both created and destroyed during post-fire debris flows in Big Creek. These jams starve downstream reaches of sediment, as exemplified in our SfM study reaches in Big Creek downstream of the log jam at the Brunette Creek confluence; in turn, low sediment supply accelerates recovery toward previously sediment-starved conditions.

As anthropogenic climate change continues to increase the frequency of post-fire disturbance events and high-resolution geomorphic data sets become more widely available, so too will opportunities to characterize and quantify post-fire geomorphic change in fluvial systems.

Data Availability Statement

Structure from Motion orthoimagery, lidar differencing products, and grain size data are available in Olsen and Pfeiffer (2024).

Acknowledgments

This work was funded by the Geological Society of America, the National Center for Airborne Laser Mapping, the Washington Section of the American Water Resources Association, the Western Washington University Research and Sponsored Programs Office, and the Western Washington University Geology Department. Chuxuan Li and Daniel E. Horton were supported by NSF PREEVENTS Grant 1854951. We thank Ed Fordham, Charlie Vryhof, Colin Dechenne, and Isaac Apaez-Guttierez for providing integral field and laboratory assistance. We are grateful to Scott Walls, who installed a network of GPS control points in Big Creek, which greatly improved the accuracy and efficiency of 2022 field surveys. We are also indebted to Mark Readdie and the staff at Big Creek Reserve who provided support for our field work. We thank Dr. Thomas Williams, Dr. Dave Rundio, Dr. Colin Amos, and Dr. Alexander Handwerger, who provided thoughtful feedback and discussion for this work. The associate editor and three anonymous reviewers provided detailed, constructive feedback, which greatly improved the quality of this manuscript.

References

AghaKouchak, A., Huning, L. S., Sadegh, M., Qin, Y., Markonis, Y., Vahedifard, F., et al. (2023). Toward impact-based monitoring of drought and its cascading hazards. *Nature Reviews Earth & Environment*, *4*(8), 582–595. https://doi.org/10.1038/s43017-023-00457-2

Bailey, P., Wheaton, J., Reimer, M., & Brasington, J. (2020). Geomorphic change detection software (version 7.5.0) [Software]. *Zenodo*. https://doi.org/10.5281/ZENODO.7248344

Bunte, K., & Abt, S. R. (2001). Sampling surface and subsurface particle-size distributions in wadable gravel-and cobble-bed streams for analyses in sediment transport, hydraulics, and streambed monitoring (No. RMRS-GTR-74) (p. RMRS-GTR-74). *U.S. Department of Agriculture, Forest Service, Rocky Mountain Research Station*. https://doi.org/10.2737/RMRS-GTR-74

Cannon, S. H. (2001). Debris-flow generation from recently burned watersheds. *Environmental and Engineering Geoscience*, *7*(4), 321–341. https://doi.org/10.2113/gseegeosci.7.4.321

Canovaro, F., Paris, E., & Solari, L. (2004). Influence of macro-roughness arrangement on flow regime. In M. Greco, A. Caravetta, & R. Della Morte (Eds.), *River flow 2004* (pp. 287–293). Taylor and Francis.

Cayan, D. R., Maurer, E. P., Dettinger, M. D., Tyree, M., & Hayhoe, K. (2008). Climate change scenarios for the California region. *Climatic Change*, *87*(S1), 21–42. https://doi.org/10.1007/s10584-007-9377-6

Cenderelli, D. A., & Kite, J. S. (1998). Geomorphic effects of large debris flows on channel morphology at North Fork Mountain, eastern West Virginia, USA. *Earth Surface Processes and Landforms: The Journal of the British Geomorphological Group*, *23*(1), 1–19. https://doi.org/10.1002/(sici)1096-9837(199801)23:1<1::aid-esp814>3.0.co;2-3

Chin, A., & Wohl, E. (2005). Toward a theory for step pools in stream channels. *Progress in Physical Geography: Earth and Environment*, *29*(3), 275–296. https://doi.org/10.1191/0309133305pp449ra

Church, M. (2006). Bed material transport and the morphology of alluvial river channels. *Annual Review of Earth and Planetary Sciences*, *34*(1), 325–354. https://doi.org/10.1146/annurev.earth.33.092203.122721

Church, M., & Jakob, M. (2020). What is a debris flood? *Water Resources Research*, *56*(8), e2020WR027144. https://doi.org/10.1029/2020WR027144

Church, M., & Zimmermann, A. (2007). Form and stability of step-pool channels: Research progress. *Water Resources Research*, *43*(3), W03415. https://doi.org/10.1029/2006WR005037

CloudCompare (version 2.13). (2023). CloudCompare (version 2.13) [GPL software]. http://www.cloudcompare.org/

DeBano, L. F. (2000). Water repellency in soils: A historical overview. *Journal of Hydrology*, *231–232*, 4–32. https://doi.org/10.1016/S0022-1694(00)00180-3

de Jonge, L., Jacobsen, O., & Moldrup, P. (1999). Soil water repellency: Effects of water content, temperature, and particle size. *Soil Science Society of America Journal - SSSAJ*, *63*(3), 437–442. https://doi.org/10.2136/sssaj1999.03615995006300030003x

Dettinger, M. D. (2013). Atmospheric rivers as drought busters on the U.S. West coast. *Journal of Hydrometeorology*, *14*(6), 1721–1732. https://doi.org/10.1175/JHM-D-13-02.1

Dettinger, M. D., Ralph, F. M., Das, T., Neiman, P. J., & Cayan, D. R. (2011). Atmospheric rivers, floods and the water Resources of California. *Water*, *3*(2), 445–478. https://doi.org/10.3390/w3020445

Dibblee, T. W., Jr. (1974). Geologic maps of the monterey, salinas, gonzales, point Sur, Jamesburg, Soledad, and Junipero Serra 15' quadrangles. *USGS Open-File Report*. https://doi.org/10.3133/ofr741021

DiBiase, R. A., & Lamb, M. P. (2013). Vegetation and wildfire controls on sediment yield in bedrock landscapes. *Geophysical Research Letters*, *40*(6), 1093–1097. https://doi.org/10.1002/grl.50277

DiBiase, R. A., & Lamb, M. P. (2020). Dry sediment loading of headwater channels fuels post-wildfire debris flows in bedrock landscapes. *Geology*, *48*(2), 189–193. https://doi.org/10.1130/g46847.1

Dietrich, W. E., Kirchner, J. W., Ikeda, H., & Iseya, F. (1989). Sediment supply and the development of the coarse surface layer in gravel-bedded rivers. *Nature*, *340*(6230), 215–217. https://doi.org/10.1038/340215a0

Dietrich, W. E., Nelson, P. A., Yager, E., Venditti, J. G., Lamb, M. P., & Collins, L. (2005). Sediment patches, sediment supply, and channel morphology. *River Coastal and Estuarine Morphodynamics*, 79–90.

Diffenbaugh, N. S., Swain, D. L., & Touma, D. (2015). Anthropogenic warming has increased drought risk in California. *Proceedings of the National Academy of Sciences*, *112*(13), 3931–3936. https://doi.org/10.1073/pnas.1422385112

East, A. E., Harrison, L. R., Smith, D. P., Logan, J. B., & Bond, R. M. (2023). Six years of fluvial response to a large dam removal on the Carmel River, California, USA. *Earth Surface Processes and Landforms*, *48*(8), 1487–1501. https://doi.org/10.1002/esp.5561

East, A. E., & Sankey, J. B. (2020). Geomorphic and sedimentary effects of modern climate change: Current and anticipated future conditions in the western United States. *Reviews of Geophysics*, *58*(4), e2019RG000692. https://doi.org/10.1029/2019RG000692

Eaton, B. C., MacKenzie, L. G., & Booker, W. H. (2020). Channel stability in steep gravel–cobble streams is controlled by the coarse tail of the bed material distribution. *Earth Surface Processes and Landforms*, *45*(14), 3639–3652. https://doi.org/10.1002/esp.4994

Eldardiry, H., Mahmood, A., Chen, X., Hossain, F., Nijssen, B., & Lettenmaier, D. P. (2019). Atmospheric river–induced precipitation and snowpack during the western United States cold season. *Journal of Hydrometeorology*, *20*(4), 613–630. https://doi.org/10.1175/jhm-d-18-0228.1

Ennos, A. R., & van Casteren, A. (2009). Transverse stresses and modes of failure in tree branches and other beams. *Proceedings of the Royal Society B: Biological Sciences*, *277*(1685), 1253–1258. https://doi.org/10.1098/rspb.2009.2093

Everest, F. H., & Meehan, W. R. (1981). Forest management and anadromous fish habitat productivity. *Transactions of the 46th North American Wildlife and Natural Resources Conference*, *10*.

Florsheim, J. L., Chin, A., Kinoshita, A. M., & Nourbakhshbeidokhti, S. (2017). Effect of storms during drought on post-wildfire recovery of channel sediment dynamics and habitat in the southern California chaparral, USA. *Earth Surface Processes and Landforms*, *42*(10), 1482–1492. https://doi.org/10.1002/esp.4117

Florsheim, J. L., Keller, E. A., & Best, D. W. (1991). Fluvial sediment transport in response to moderate storm flows following chaparral wildfire, Ventura County, southern California. *Geological Society of America Bulletin*, *103*(4), 504–511. https://doi.org/10.1130/0016-7606(1991)103<0504:fstirt>2.3.co;2

Gabet, E. J., & Sternberg, P. (2008). The effects of vegetative ash on infiltration capacity, sediment transport, and the generation of progressively bulked debris flows. *Geomorphology*, *101*(4), 666–673. https://doi.org/10.1016/j.geomorph.2008.03.005

Gran, K. B., & Montgomery, D. R. (2005). Spatial and temporal patterns in fluvial recovery following volcanic eruptions: Channel response to basin-wide sediment loading at Mount Pinatubo, Philippines. *GSA Bulletin*, *117*(1–2), 195–211. https://doi.org/10.1130/B25528.1

Griffin, D., & Anchukaitis, K. J. (2014). How unusual is the 2012–2014 California drought? *Geophysical Research Letters*, *41*(24), 9017–9023. https://doi.org/10.1002/2014GL062433

Harrison, L. R., East, A. E., Smith, D. P., Logan, J. B., Bond, R. M., Nicol, C. L., et al. (2018). River response to large-dam removal in a Mediterranean hydroclimatic setting: Carmel River, California, USA: River response to large-dam removal. *Earth Surface Processes and Landforms*, *43*(15), 3009–3021. https://doi.org/10.1002/esp.4464

Hassan, M. A., Saletti, M., McDowell, C., & Li, W. (2023). Sediment dynamics and bed stability in step-pool streams: Insights from 18 Years of field observations. *Water Resources Research*, *59*(1), e2022WR032864. https://doi.org/10.1029/2022WR032864

Hecht, C. W., & Cordeira, J. M. (2017). Characterizing the influence of atmospheric river orientation and intensity on precipitation distributions over North Coastal California. *Geophysical Research Letters*, *44*(17), 9048–9058. https://doi.org/10.1002/2017GL074179

Henson, P., & Usner, D. J. (1996). *The natural history of Big Sur*. University of California Press.

Hoell, A., Quan, X.-W., Hoerling, M., Fu, R., Mankin, J., Simpson, I., et al. (2022). Record low north American monsoon rainfall in 2020 reignites drought over the American southwest. *Bulletin of the American Meteorological Society*, *103*(3), S26–S32. https://doi.org/10.1175/BAMS-D-21-0129.1

Hoffman, D. F., & Gabet, E. J. (2007). Effects of sediment pulses on channel morphology in a gravel-bed river. *Geological Society of America Bulletin*, *119*(1–2), 116–125. https://doi.org/10.1130/B25982.1

Ice, G. G., Neary, D. G., & Adams, P. W. (2004). Effects of wildfire on soils and watershed processes. *Journal of Forestry*, *102*(6), 16–20. https://doi.org/10.1093/jof/102.6.16

Jackson, L. E., Kostaschuk, R. A., & MacDonald, G. M. (1987). Identification of debris flow hazard on alluvial fans in the Canadian Rocky Mountains. *Debris flows/avalanches: process, recognition, and mitigation*, 115–124. https://doi.org/10.1130/reg7-p115

Jarrett, R. D. (1984). Hydraulics of high-gradient streams. *Journal of Hydraulic Engineering*, *110*(11), 1519–1539. https://doi.org/10.1061/(ASCE)0733-9429(1984)110:11(1519)

Johnston, S. M., Singleton, J. S., Chapman, A. D., & Murray, G. (2018). Geologic map and structural development of the northernmost Sur-Nacimiento fault zone, central California coast. *Geosphere*, *15*(1), 171–187. https://doi.org/10.1130/GES02015.1

Keller, E. A., Bean, G., & Best, D. (2015). Fluvial geomorphology of a boulder-bed, debris-flow—Dominated channel in an active tectonic environment. *Geomorphology*, *243*, 14–26. https://doi.org/10.1016/j.geomorph.2015.04.012

Kemp, P., Sear, D., Collins, A., Naden, P., & Jones, I. (2011). The impacts of fine sediment on riverine fish. *Hydrological Processes*, *25*(11), 1800–1821. https://doi.org/10.1002/hyp.7940

Kinoshita, A., & Hogue, T. (2011). Spatial and temporal controls on post-fire hydrologic recovery in southern California watersheds. *Fuel and Energy Abstracts*, *87*(2), 240–252. https://doi.org/10.1016/j.catena.2011.06.005

Kondolf, G. M., & Wolman, M. G. (1993). The sizes of salmonid spawning gravels. *Water Resources Research*, *29*(7), 2275–2286. https://doi.org/10.1029/93WR00402

Lamb, M. P., Levina, M., DiBiase, R. A., & Fuller, B. M. (2013). Sediment storage by vegetation in steep bedrock landscapes: Theory, experiments, and implications for postfire sediment yield. *Journal of Geophysical Research: Earth Surface*, *118*(2), 1147–1160. https://doi.org/10.1002/jgrf.20058

Lenzi, M. A., Mao, L., & Comiti, F. (2006). Effective discharge for sediment transport in a mountain river: Computational approaches and geomorphic effectiveness. *Journal of Hydrology*, *326*(1–4), 257–276. https://doi.org/10.1016/j.jhydrol.2005.10.031

Li, C., Handwerger, A. L., Wang, J., Yu, W., Li, X., Finnegan, N. J., et al. (2022). Augmentation of WRF-Hydro to simulate overland-flow- and streamflow-generated debris flow susceptibility in burn scars. *Natural Hazards and Earth System Sciences*, *22*(7), 2317–2345. https://doi.org/10.5194/nhess-22-2317-2022

Lisle, T. (1987). Overview: Channel morphology and sediment transport in steepland streams. *Erosion and Sedimentation in the Pacific Rim (Proceedings of the Corvailis Symposium, August, 1987)*.

Lisle, T. E., & Hilton, S. (1992). The volume of fine sediment in pools: An index of sediment supply in gravel-bed Streams1. *JAWRA Journal of the American Water Resources Association*, *28*(2), 371–383. https://doi.org/10.1111/j.1752-1688.1992.tb04003.x

Liu, T., McGuire, L. A., Wei, H., Rengers, F. K., Gupta, H., Ji, L., & Goodrich, D. C. (2021). The timing and magnitude of changes to Hortonian overland flow at the watershed scale during the post-fire recovery process. *Hydrological Processes*, *35*(5), e14208. https://doi.org/10.1002/hyp.14208

Loáiciga, H. A., Pedreros, D., & Roberts, D. (2001). Wildfire-streamflow interactions in a chaparral watershed. *Advances in Environmental Research*, *5*(3), 295–305. https://doi.org/10.1016/S1093-0191(00)00064-2

MacDonald, L. H., & Huffman, E. L. (2004). Post-fire soil water repellency: Persistence and soil moisture thresholds. *Soil Science Society of America Journal*, *68*(5), 1729–1734. https://doi.org/10.2136/sssaj2004.1729

MacKenzie, L. G., & Eaton, B. C. (2017). Large grains matter: Contrasting bed stability and morphodynamics during two nearly identical experiments. *Earth Surface Processes and Landforms*, *42*(8), 1287–1295. https://doi.org/10.1002/esp.4122

Major, J. J., East, A. E., O'Connor, J. E., Grant, G. E., Wilcox, A. C., Magirl, C. S., et al. (2017). Geomorphic responses to dam removal in the United States - A two-decade perspective. In D. Tsutsumi & J. B. Laronne (Eds.), *Gravel-bed rivers* (pp. 355–383). John Wiley & Sons, Ltd. https://doi.org/10.1002/9781118971437.ch13

Mao, L., Uyttendaele, G. P., Iroumé, A., & Lenzi, M. A. (2008). Field based analysis of sediment entrainment in two high gradient streams located in Alpine and Andine environments. *Geomorphology*, *93*(3–4), 368–383. https://doi.org/10.1016/j.geomorph.2007.03.008

McGuire, L. A., Rengers, F. K., Kean, J. W., & Staley, D. M. (2017). Debris flow initiation by runoff in a recently burned basin: Is grain-by-grain sediment bulking or en masse failure to blame? *Geophysical Research Letters*, *44*(14), 7310–7319. https://doi.org/10.1002/2017GL074243

Meyer, G., & Wells, S. G. (1997). Fire-Related Sedimentation Events on Alluvial Fans, Yellowstone National Park, U.S.A. *SEPM Journal of Sedimentary Research*, *67*. https://doi.org/10.1306/D426863A-2B26-11D7-8648000102C1865D

Montgomery, D. R., & Buffington, J. M. (1997). Channel-reach morphology in mountain drainage basins. *Geological Society of America Bulletin*, *109*(5), 596–611. https://doi.org/10.1130/0016-7606(1997)109<0596:crmimd>2.3.co;2

Morell, K. D., Alessio, P., Dunne, T., & Keller, E. (2021). Sediment Recruitment and Redistribution in Mountain Channel Networks by Post-Wildfire Debris Flows. *Geophysical Research Letters*, *48*(24), e2021GL095549. https://doi.org/10.1029/2021GL095549

Nyman, P., Smith, H. G., Sherwin, C. B., Langhans, C., Lane, P. N. J., & Sheridan, G. J. (2015). Predicting sediment delivery from debris flows after wildfire. *Geomorphology*, *250*, 173–186. https://doi.org/10.1016/j.geomorph.2015.08.023

Olsen, T. (2023). *Quantifying Channel change following post-fire debris flows in a steep, coastal stream, Big Sur* (Vol. 1256). WWU Graduate School Collection.

Olsen, T., & Pfeiffer, A. (2024). Impacts of Post-fire Debris Flows on Fluvial Morphology and Sediment Transport in a California Central Coast Stream [Dataset]. *Zenodo*. https://doi.org/10.5281/zenodo.10514493

OpenTopography. (2013). California Coast: Big Creek, Vincente, Arroyo Seco, Scotts Creek, UCSC [Dataset]. https://doi.org/10.5069/G9SQ8XB0

OpenTopography. (2016). Big Creek [Dataset]. https://doi.org/10.5069/G91V5BX0

OpenTopography. (2023). Quantifying Channel Change in a Steep Coastal Stream, CA 2022 [Dataset]. https://doi.org/10.5069/G9TD9VJF

Paola, C., & Mohrig, D. (1996). Palaeohydraulics revisited: Palaeoslope estimation in coarse-grained braided rivers. *Basin Research*, *8*(3), 243–254. https://doi.org/10.1046/j.1365-2117.1996.00253.x

Parker, G. (1990). Surface-based bedload transport relation for Gravel Rivers. *Journal of Hydraulic Research*, *28*(4), 417–436. https://doi.org/10.1080/00221689009499058

Persad, G. G., Swain, D. L., Kouba, C., & Ortiz-Partida, J. P. (2020). Inter-model agreement on projected shifts in California hydroclimate characteristics critical to water management. *Climatic Change*, *162*(3), 1493–1513. https://doi.org/10.1007/s10584-020-02882-4

Prancevic, J. P., & Lamb, M. P. (2015). Particle friction angles in steep mountain channels. *Journal of Geophysical Research: Earth Surface*, *120*(2), 242–259. https://doi.org/10.1002/2014JF003286

Purinton, B., & Bookhagen, B. (2019). Introducing PebbleCounts: A grain-sizing tool for photo surveys of dynamic gravel-bed rivers. *Earth Surface Dynamics*, *7*(3), 859–877. https://doi.org/10.5194/esurf-7-859-2019

Purinton, B., & Bookhagen, B. (2021). Tracking Downstream Variability in Large Grain-Size Distributions in the South-Central Andes. *Journal of Geophysical Research: Earth Surface*, *126*(8), e2021JF006260. https://doi.org/10.1029/2021JF006260

Recking, A. (2013). Simple Method for Calculating Reach-Averaged Bed-Load Transport. *Journal of Hydraulic Engineering*, *139*(1), 70–75. https://doi.org/10.1061/(ASCE)HY.1943-7900.0000653

Rengers, F. K., McGuire, L. A., Barnhart, K. R., Youberg, A. M., Cadol, D., Gorr, A. N., et al. (2023). The influence of large woody debris on post-wildfire debris flow sediment storage. *Natural Hazards and Earth System Sciences*, *23*(6), 2075–2088. https://doi.org/10.5194/nhess-23-2075-2023

Rengers, F. K., McGuire, L. A., Kean, J. W., Staley, D. M., Dobre, M., Robichaud, P. R., & Swetnam, T. (2021). Movement of Sediment Through a Burned Landscape: Sediment Volume Observations and Model Comparisons in the San Gabriel Mountains, California, USA. *Journal of Geophysical Research: Earth Surface*, *126*(7), e2020JF006053. https://doi.org/10.1029/2020JF006053

Riebe, C. S., Sklar, L. S., Overstreet, B. T., & Wooster, J. K. (2014). Optimal reproduction in salmon spawning substrates linked to grain size and fish length. *Water Resources Research*, *50*(2), 898–918. https://doi.org/10.1002/2013WR014231

Scheingross, J. S., Winchell, E. W., Lamb, M. P., & Dietrich, W. E. (2013). Influence of bed patchiness, slope, grain hiding, and form drag on gravel mobilization in very steep streams. *Journal of Geophysical Research: Earth Surface*, *118*(2), 982–1001. https://doi.org/10.1002/jgrf.20067

Short, L. E., Gabet, E. J., & Hoffman, D. F. (2015). The role of large woody debris in modulating the dispersal of a post-fire sediment pulse. *Geomorphology*, *246*, 351–358. https://doi.org/10.1016/j.geomorph.2015.06.031

Stock, J. D., & Dietrich, W. E. (2006). Erosion of steepland valleys by debris flows. *GSA Bulletin*, *118*(9–10), 1125–1148. https://doi.org/10.1130/B25902.1

Stoof, C. R., Vervoort, R. W., Iwema, J., van den Elsen, E., Ferreira, A. J. D., & Ritsema, C. J. (2012). Hydrological response of a small catchment burned by experimental fire. *Hydrology and Earth System Sciences*, *16*(2), 267–285. https://doi.org/10.5194/hess-16-267-2012

Swain, D. L., Langenbrunner, B., Neelin, J. D., & Hall, A. (2018). Increasing precipitation volatility in twenty-first-century California. *Nature Climate Change*, *8*(5), 427–433. https://doi.org/10.1038/s41558-018-0140-y

Tietje, W. D., Preston, W. L., & Polyakov, A. Y. (2019). California Naturalist Series: Natural History of the Central Coast Bioregion. *University of California, Agriculture and Natural Resources*. https://doi.org/10.3733/ucanr.8597

U.S. Forest Service. (2020). Dolan Fire Burned-Area Report.

Wagenbrenner, J. W., Ebel, B. A., Bladon, K. D., & Kinoshita, A. M. (2021). Post-wildfire hydrologic recovery in Mediterranean climates: A systematic review and case study to identify current knowledge and opportunities. *Journal of Hydrology*, *602*, 126772. https://doi.org/10.1016/j.jhydrol.2021.126772

Wang, J., Hassan, M. A., Saletti, M., Chen, X., Fu, X., Zhou, H., & Yang, X. (2021). On How Episodic Sediment Supply Influences the Evolution of Channel Morphology, Bedload Transport and Channel Stability in an Experimental Step-Pool Channel. *Water Resources Research*, *57*(7), e2020WR029133. https://doi.org/10.1029/2020WR029133

Wilcock, P. R., & Crowe, J. C. (2003). Surface-based transport model for mixed-size sediment. *Journal of Hydraulic Engineering*, *129*(2), 120–128. https://doi.org/10.1061/(asce)0733-9429(2003)129:2(120)

Wilford, D., Sakals, M., Innes, J., Sidle, R., & Bergerud, W. A. (2004). Recognition of debris flow, debris flood and flood hazard through watershed morphometrics. *Landslides*, *1*, 61–66. https://doi.org/10.1007/s10346-003-0002-0

Williams, A. P., Abatzoglou, J. T., Gershunov, A., Guzman-Morales, J., Bishop, D. A., Balch, J. K., & Lettenmaier, D. P. (2019). Observed impacts of anthropogenic climate change on wildfire in California. *Earth's Future*, *7*(8), 892–910. https://doi.org/10.1029/2019ef001210

Williams, A. P., Seager, R., Abatzoglou, J. T., Cook, B. I., Smerdon, J. E., & Cook, E. R. (2015). Contribution of anthropogenic warming to California drought during 2012–2014. *Geophysical Research Letters*, *42*(16), 6819–6828. https://doi.org/10.1002/2015GL064924

Yager, E. M., Dietrich, W. E., Kirchner, J. W., & McArdell, B. W. (2012). Prediction of sediment transport in step-pool channels. *Water Resources Research*, *48*(1), W01541. https://doi.org/10.1029/2011WR010829

Yager, E. M., Kirchner, J. W., & Dietrich, W. E. (2007). Calculating bed load transport in steep boulder bed channels. *Water Resources Research*, *43*(7), W07418. https://doi.org/10.1029/2006WR005432

Young, H. H., & Hilley, G. E. (2018). Millennial-scale denudation rates of the Santa Lucia Mountains, California: Implications for landscape evolution in steep, high-relief, coastal mountain ranges. *GSA Bulletin*, *130*(11–12), 1809–1824. https://doi.org/10.1130/B31907.1

Zimmermann, A., & Church, M. (2001). Channel morphology, gradient profiles and bed stresses during flood in a step–pool channel. *Geomorphology*, *40*(3–4), 311–327. https://doi.org/10.1016/S0169-555X(01)00057-5